1,2,4-Triazolo[1,5-a]quinoxaline derivatives and their simplified analogues as adenosine A3 receptor antagonists. Synthesis, structure–affinity relationships and molecular modeling studies

Daniela Catarzi [a,*], Flavia Varano [a], Daniela Poli [a], Lucia Squarcialupi [a], Marco Betti [a], Letizia Trincavelli [b], Claudia Martini [b], Diego Dal Ben [c], Ajiroghene Thomas [c], Rosaria Volpini [c], Vittoria Colotta [a]

[a] *Dipartimento di Neuroscienze, Psicologia, Area del Farmaco e Salute del Bambino, Sezione di Farmaceutica e Nutraceutica, Università di Firenze, Polo Scientifico, Via Ugo Schiff 6, 50019 Sesto Fiorentino, FI, Italy*
[b] *Dipartimento di Farmacia, Università di Pisa, Via Bonanno Pisano 6, 56126 Pisa, Italy*
[c] *School of Pharmacy, Medicinal Chemistry Unit, University of Camerino, Via S. Agostino 1, 62032 Camerino (MC), Italy*

doi: 10.1016/j.bmc.2014.11.033

* Corresponding author. Tel.: +39 055 4573722; fax: +39 055 4573780.

E-mail address: daniela.catarzi@unifi.it (D. Catarzi)DOI: 10.1016/j.ejmech.2014.10.020

Abstract

The 1,2,4-triazolo[1,5-a]quinoxaline (TQX) scaffold was extensively investigated in our previously reported studies and recently, our attention was focused at position 5 of the tricyclic nucleus where different acyl and carboxylate moieties were introduced (compounds 2–15). This study produced some interesting compounds endowed with good hA3 receptor affinity and selectivity. In addition, to find new insights about the structural requirements for hA3 receptor–ligand interaction, the tricyclic TQX ring was destroyed yielding some 1,2,4-triazole derivatives (compounds 16–23). These simplified compounds, though maintaining the crucial structural requirements for adenosine receptor–ligand interaction, have a very low hA3 adenosine receptor affinity, the only exception being compound 23 (1-[3-(4-methoxyphenyl)-1-phenyl-1H-1,2,4-triazol-5-yl]-3-phenylurea) endowed with a Ki value in the micro-molar range and high hA3 selectivity versus both hA1 and hA2A AR subtypes. Evaluation of the side products obtained in the herein reported synthetic pathways led to the identification of some new triazolo[1,5-a]quinoxalines as hA3AR antagonists (compounds 24–27). These derivatives, though lacking the classical structural requirements for the anchoring at the hA3 receptor site, show high hA3 affinity and in some case selectivity versus hA1 and hA2A subtypes. Molecular docking of the herein reported tricyclic and simplified derivatives was carried out to depict their hypothetical binding mode to our model of hA3 receptor.

Keywords:

G protein-coupled receptors; Adenosine receptor antagonists; Triazoloquinoxalines; Tricyclic heteroaromatic systems; Ligand–receptor modeling studies.

1. Introduction

Adenosine is a ubiquitous nucleoside that regulates a large number of physiological and patho-physiological processes by triggering specific adenosine receptors (ARs) at the extracellular level. The ARs are four different subtypes of G protein-coupled receptors (GPCRs) classified as A1, A2A, A2B and A3 on the basis of their tissue localization, respective coupling to adenylate cyclase (AC) and specific pharmacological criteria.1

The adenosine A3 receptor (A3AR), the most recently characterized, was originally isolated from rat testis2 and subsequently cloned from a variety of species.3 For the A3AR, significant differences (72%) in sequence similarity and tissue distribution have been observed between species.4,5 However, this receptor is widely distributed in the human body, both in peripheral organs and in distinct regions of the central nervous system (CNS), though in low levels. The A3AR is reported to be related to various second messenger systems. Its activation leads to inhibition of AC and stimulation of phospholipase C and D6,7 through Gi and Gq proteins, respectively. Moreover, additional intracellular pathways have been described to be important for intracellular signal transduction in the adenosine biochemical system.6,8 The improved understanding of the physiological effects mediated by the A3AR and of its biology has provided substantial evidence that this AR subtype is an interesting target for different therapeutic interventions. In particular, A3AR antagonists are being investigated for the treatment of glaucoma, asthma, inflammation9 and cerebral ischemia.10,11 A3AR antagonists have also been reported to have potential efficacy in both glioblastoma multiforme and colon cancer therapy.12,13

However, the role of A3AR antagonists as potential therapeutics in many pathological diseases such as inflammation, cerebral ischemia and cancer is still ambiguous and widely debated.14 Thus, the search for potent and selective human (h) A3AR antagonists has become an attractive

goal for many scientists. In the last few years, much effort has been directed toward design and development of potent and selective AR antagonists belonging to diverse classes of heterocyclic derivatives with different structures.9

The 1,2,4-triazolo[1,5-a]quinoxaline (TQX) ring system is a recurrent structural core which has been used to obtain tricyclic AR antagonists.15–18 The first AR antagonists belonging to this series were designed as structural analogues of CGS15943 (9-chloro-2-(2-furanyl)[1,2,4]triazolo[1,5-c]quinazolin-5-amine)19 in the midnineties15 and, since then, many other TQX derivatives of interest have been developed by our research group. In particular, the 8-chloro-2-phenyl-1,2,4-triazolo[1,5-a]quinoxalin-4-amine17 (1A, Fig. 1) was modified by introducing suitable substituents either on the 4-amino group or the 2-phenyl ring (Series A,17 Fig. 1). The presence of an acyl moiety on the 4-amino group, as in compound 2A, led to potent and selective hA3AR antagonists. The improvement of hA3 affinity and selectivity was hypothesized to be due to the amide carbonyl at position-4 that can act as a proton acceptor in a hydrogen bonding interaction with a proton donor binding site. A further increase in affinity was observed when a methoxy group which can engage an additional hydrogen bond with the receptor site was introduced in the para position of the 2-phenyl substituent.17

These promising results indicated that the TQX ring system is a versatile scaffold which can be further modified to develop new AR antagonists. Thus, we studied a series of 2-(hetero)aryl-1,2,4-triazolo[1,5-a]quinoxaline derivatives bearing a 4-oxo function replacing the 4-amino group of the previously reported Series A (Series B,18 Fig. 1). Some interesting hA3 AR antagonists were produced starting from the 8-chloro-2-phenyl-4,5-dihydro-1,2,4-triazolo[1,5-a]quinoxalin-4-one 1B, selected as lead compound.18 Profitable modifications were made either by introducing different aryl and heteroaryl groups at position 2, or by replacing the 8-chloro substituent with a methyl group or a hydrogen atom. In order to further investigate the

potentiality of the TQX ring system, we decided to move the 4-carbonyl function of Series B into an exonuclear position by introducing different acyl or carboxyalkyl substituents at N-5 (Series C, compounds 2–15, Fig. 2). We also introduced the above cited suitable substituents, that is, the 8-chloro or 8-methyl on the fused benzo moiety and the crucial 4-methoxy on the 2-phenyl ring, onto the TQX scaffold.

To find new insights into the structural requirements for hA3 receptor–ligand interaction, the tricyclic TQX ring was destroyed by eliminating the 4-methylene bridge of Series C, generating the new 1,3-diaryl-1,2,4-triazole monocyclic core (Series D1, compounds 16–19, Fig. 2) which can be considered a simplified structure of Series C. Contemporarily, analogues of Series D1, called Series D2 (compounds 20–23), were designed by moving the substituted NH group from the ortho-position of the 1-aryl moiety to the 5-position on the 1,2,4-triazole core. Hence, both Series D1 and D2 maintain the substituted NH group and the two aryl moieties which could be important requirements for a profitable interaction with the AR binding pockets.9 It has to be noted that only a few other monocyclic cores have been evaluated as possible candidates for developing AR antagonists.20–25

In addition, looking at the side products in the synthetic pathway which leads to the targeted TQX compounds, we have identified the 4,5-dehydro-derivatives (Series E, compounds 24–27, Figure 2) as possible candidates for our pharmacological studies. Unlike the other series herein reported, these compounds lack all the classical structural requirements considered important for anchoring at the receptor binding sites, while maintaining only the nude tricyclic TQX scaffold.

2. Chemistry

The synthetic pathways which yielded compounds 2–15, 16–19, 20–23 and 24–2726 are illustrated in Schemes 1–3. Compounds 2–15 (Series C) were obtained starting from the 2-aryl-4,5-dihydro- 1,2,4-triazolo[1,5-a]quinoxalin-4-ones 28–31,18,26 as reported in Scheme 1.

Reduction of the 4-oxo function of 28–31 with LiAlH4 led to a mixture of the key intermediates 32–3526 and small amounts of the 4,5-dehydro-derivatives 24–27,26 which were successively evaluated as AR antagonists. An increased quantity of 25 and 27 was obtained by treating 33 and 35, respectively, with glacial acetic acid at reflux. Derivatives 32–35 were reacted with the suitable acyl chloride or chloroformates in the presence of pyridine to yield the final N-5-substituted compounds 2–15. In order to find an alternative synthetic pathway to achieve the target compounds 32–35 with higher yields, we synthesized 35 starting from the 1,3-diaryl-5-chloromethyl-1,2,4-triazole 37 which was obtained by treating the amidrazone 3618 with chloroacetyl chloride. The intermediate 37 was transformed into the tricyclic derivative 35 with SnCl2 dihydrate, and only traces of compound 27 were obtained (1H NMR determination). In this way the synthetic procedure for preparing 35 has been shortened and the total yield improved.

The simplified 1,2,4-triazole derivatives of Series D1 (16–19) were obtained as reported in Scheme 2. Reaction of 36 with triethyl orthoformate in the presence of para-toluenesulfonic acid, led to 1,2,4-triazole cyclization (compound 38). By reduction of the nitro group of 38, the corresponding amino-derivative 39 was obtained which was reacted with the suitable acyl chloride or chloroformates to provide compounds 16–19 with high yields.

The synthesis of compounds 20–23 (Series D2) was performed as reported in Scheme 3. By reacting the hydrazide 4027,28 with a mixture of POCl3 and PCl5 at reflux, the unstable chloroimine 4129 was obtained which was immediately reacted with cyanamide at 100 °C in solvent-free conditions to give the intermediate 42. Then, the latter was transformed into the corresponding acyland carbamoyl-derivatives by reacting with acetic anhydride (compound 20), benzoyl chloride (21, 22) or phenyl isocyanate (23).

3. Pharmacology

The newly synthesized derivatives 2–15 (Table 1), 16–23 (Table 2), and 24–27 (Table 3) were tested for their ability to displace [125I]N6-(4-amino-3-iodobenzyl)-50-(N-methylcarbamoyl) adenosine ([125I]AB-MECA) from a cloned hA3 receptor stably expressed in CHO cells. Subsequently, all compounds except 3 and 25, were evaluated for their ability to displace [3H]8-cyclopentyl-1,3-dipropylxantine ([3H]DPCPX) from cloned hA1 ARs, and [3H]50-(N-ethylcarboxamido)adenosine ([3H]NECA) from cloned hA2A ARs, to establish their A3 versus A1 and versus A2A selectivity. In Table 1, the binding results of the reference compound 1B18 (Fig. 1) at hA3 AR is reported. To determine hA3 versus hA2B selectivity, some selected compounds (2, 7–9, 11, 13–14, 27) were tested at the hA2B subtype by measuring their effects on cyclic adenosine monophosphate (cAMP) accumulation in CHO cells stably transfected with the hA2B AR (Table 4).

4. Results and discussion

4.1. Structure–affinity relationships

The binding results reported in Tables 1–3 indicate that we have produced some new potent and selective hA3 AR antagonists belonging to the 1,2,4-triazolo[1,5-a]quinoxaline series (Series C and E, Table 1 and 3, respectively). Some of the novel derivatives show high hA3 AR affinity (Ki <100 nM) and selectivity versus the hA2A receptor (compounds 2, 7–9 and 11–14) and, in some cases, also good selectivity versus the hA1 subtype. The choice to test the side products 24–27 (Series E, Table 3) which turned out to be potent hA3AR antagonists and, in the case of 26 and 27 also selective versus both the hA1 and hA2A subtypes in the binding assays was fortunate. In contrast, the simplified 1,2,4-triazole derivatives (Series D1 and D2, Table 2) were inactive or had very low activity at all the AR subtypes, the only exception being compound 23

endowed with a Ki value at the hA3AR in the micromolar range and high selectivity versus both hA1 and hA2A subtypes.

Focusing on the results reported in Table 1, we can observe that elimination of the 8-chloro substituent is detrimental for hA3 receptor–ligand interaction (compare 2 and 3 to 4 and 6, respectively), while its replacement with a methyl group leads to a strong increase in hA3 affinity (compare compounds 7 and 9 to 2 and 3, respectively) and maintains good hA3 selectivity versus both hA1 and hA2A receptors. High hA3 AR binding activity is also observed for compounds 11–14 which hold the methyl group at position 8 but, unlike derivatives 7–10, are decorated with a para-methoxy group on the 2-phenyl ring. These modifications maintain very high selectivity versus both the hA2A and the hA1 ARs, the only exception being compound 12 which shows, compared to the parent 9, a dramatic increase in hA1 AR affinity and a total loss of hA3 versus hA1 selectivity. Nevertheless, the introduction of the paramethoxy group does not exert the positive effect on hA3 affinity observed in the previously reported Series A and B17,18 (Fig. 1). In fact, it has to be noted that compounds 11 and 12 possess a 3-fold reduced hA3 affinity compared to 7 and 9.

A comparison of the binding data of the previously reported 1B (Fig. 1) with those of the 5-substituted herein reported (compounds 2–15) highlights that the hA3 binding affinities of 2–15 are similar or higher than that of 1B, with the only exceptions being the 8-unsubstituted derivatives 4, 5 and 6 and compound 15 which are less active. These data suggest that replacement of the 4-carbonyl function of Series B with exonuclear acyl or carboxyalkyl groups is well tolerated by the hA3 receptor.

The effect on hA3 AR affinity and selectivity exerted by the substituents inserted at position 5 of the TQX scaffold is very difficult to explain. By restricting our attention to the 8-methyl substituted compounds 7–15, we can observe that the binding affinity is maintained in the

nanomolar range apart from the nature of the substituent at position-5. Hence, the steric hindrance at this position does not seem to be critical for receptor–ligand interaction. It is worth noting that the 5-N-propionyl substituted derivative 7 is the most active compound at the hA3 AR with a Ki value of 6.5 nM (Table 1). Furthermore, compound 13, bearing the propargyl carboxylate group at the same position, is about 3.5-fold less active than 7, but much more selective versus the hA1 subtype.

The opening of the tricyclic TQX scaffold of Series C to produce the 1,3-diaryl-1,2,4-triazole system (Series D1, Table 2) is detrimental for hA3 AR affinity, although the resulting compounds (16–19) maintain some ability to bind the hA3 subtype (35 < I% < 50). Similar results were obtained when the substituted amino group was moved from the 1-aryl-moiety of Series D1 to the 5-position of the 1,2,4-triazole core (compounds 20–23, Series D2, Table 2). However, in contrast with the low hA3 AR affinity (19 < I% < 50) of the 5-amido-derivatives 20–22, there is the micromolar hA3 Ki value and high selectivity versus both hA1 and hA2A subtypes of compound 23. Thus, this compound could represent a suitable lead for the development of hA3 AR antagonists endowed with a small heterocyclic core.

In contrast to compounds 16–23 (Series D1 and D2), derivatives 24–27 (Series E, Table 3) hold the tricyclic ring system constant but lack both the claimed NH function and the carbonyl group which are considered important requirements for AR-ligand interaction. 9 Although these derivatives have only the endonuclear nitrogen atoms able to give hydrogen bonding interactions, they show high hA3 affinity and in some cases selectivity versus hA1 and hA2A subtypes.

This series also confirms the profitable effect of the presence of a small substituent (chloro or methyl) on the fused benzo moiety for hA3 receptor–ligand interaction. In fact, the 8-chloro- and 8-methyl-substituted compounds 24 and 26, respectively, are equipotent at the hA3AR with a Ki

value in the nanomolar range and are 4-6-fold more active than the unsubstituted derivative 25. These data suggest that these small lipophilic groups could positively interact with a hydrophobic receptor pocket. The presence of a para-methoxy substituent on the 2-phenyl ring (compound 27) is not cooperative as in Series A and B, leaving unchanged the ability to bind the hA3AR compared to compound 26.

To evaluate the hA3 versus hA2B selectivity, the affinities of some selected derivatives (2, 7–9, 11, 13–14, 27) at the hA2B AR were evaluated by cAMP functional assay using A2B transfected cells. In general, all the compounds tested alone are not effective in stimulating cAMP accumulation (data not shown). In addition, they showed low or null ability to inhibit cAMP accumulation evoked by the agonist NECA (Table 4). Thus, this study demonstrates that the tested derivatives 2, 7–9, 11, 13–14, 27 have not agonist/antagonist activity toward A2B AR subtype.

All together these data confirm that this work produced some compounds endowed with good hA3 affinity and also selectivity versus all the other ARs.

4.2. Molecular modeling studies

To define the structural features at the basis of the different binding affinities of the new derivatives, a molecular docking analysis was performed on homology models of hA3AR developed by using four X-ray structures of the antagonist-bound hA2A AR as templates (pdb code: 3EML; 2.6-Å resolution;30 pdb code: 3PWH;3.3-Å resolution;31 pdb code: 3REY; 3.3-Å resolution;31 pdb code: 3UZA; 3.3-Å resolution32). The A2AAR crystal structure provides improved accuracy of AR homology models, due to high residue conservation in the primary sequences of the AR subtypes, which share a sequence identity of ~57% within the transmembrane (TM) domains.33 The residues located within the seven TM domains in the upper part of ARs, corresponding to the ligand binding site, are conserved with an average

identity of 71%.34 Furthermore, the above cited A2AAR crystal structures have been solved in complex with high affinity antagonists (ZM241385, XAC, and the 6-(2,6-dimethylpyridin-4-yl)-5-phenyl-1,2,4-triazin-3-amine, see cited articles for details), hence presenting a cavity suitable as a binding site for docking analysis. Each obtained hA3AR homology model was checked by using the Protein Geometry Monitor application within MOE35 and then employed for a preliminary docking analysis performed by manually docking the high affinity antagonist MRS 1220 (N-[9-chloro-2-(2-furyl)[1,2,4]-triazolo[1,5-c]quinazolin-5-yl]benzene acetamide, Ki hA3AR = 0.65 nM36) structure within the respective binding site. The obtained hA3AR–MRS 1220 complexes were then subjected to energy minimization and to Monte Carlo analysis to explore the favorable binding conformations. During this analysis, the ligand was left free to be continuously re-oriented and re-positioned within the binding site and the conformation of both ligand and nearby residues could be explored and reciprocally relaxed. The remaining receptor atoms were kept fixed. This stage was crucial to provide A3AR binding sites with conformations able to accommodate the analyzed antagonists. For each A3AR model, the best receptor–MRS 1220 complex was saved and energetically minimized.

Once the MRS 1220 compound was removed, each hA3AR model was then used as target for the docking analysis of the synthesized derivatives. All ligand structures were optimized using RHF/AM1 semi-empirical calculations (with the aid of the software package MOPAC37 implemented in MOE) and then docked into the binding site of the hA3AR models by using the MOE Dock tool. Topscore docking poses of each compound were subjected to energy minimization and then rescored using three available methods implemented in MOE: the London dG scoring function, the Affinity dG scoring tool, and the dock-pKi predictor. For each compound, the four top-score docking poses, according to at least two out of three scoring functions, were selected for final ligand-target interaction analysis.

The four developed hA3AR models present highly similar binding sites by considering both pocket volumes and receptor residues orientation. In particular, the binding pockets present only subtle rearrangements of some flexible residues, while the EL domains in peripheral regions of binding site contain higher conformational variability. For example, the side chain of hA2A AR Asn250 (a critical residue for ligand interaction due to its position in the core of the binding pocket) is observed as having different conformations by comparing the hA2A AR crystal structures used as templates and analogue variability is obtained within the developed hA3AR models for the same amino acid (Asn250). Furthermore, the different interaction and distance between EL2 and EL3 domains (even due to a different orientation of Glu169) are observed in the hA2A AR X-ray structures and also in the developed hA3AR models. Consequently, it is not surprising that the docking analysis of the synthesized compounds at the four receptor models led to analogue results.

Considering the general binding mode of TQX derivatives belonging to Series C (compounds 2–15) in the hA3AR, two main sets of docking conformations were observed in all four hA3AR models. Figures 3 and 4 show the binding modes at the hA3 AR model of compounds 7 as representative of Series C compounds. The first set of conformations (from now on called 'family 1' conformations, Fig. 3, Panel A) presents the TQX moiety located in the center of the binding site with the quinoxaline ring being positioned between Phe168 (EL2) and Ile268 (TM7) side chains. The 2-substituent points towards the central transmembrane core and is located in a mainly hydrophobic subpocket in proximity of Leu90 and Leu91 (TM3), Met177 (TM5), Trp243 and Leu246 (TM6), while the fused phenyl ring is internally oriented and located in a region given by Ala69 and Val72 (TM2), Leu90 (TM3), Phe168 (EL2), and Ile268 (TM7) residues.

Superimposition of the family 1 docking conformations of each compound in the four hA3AR models shows that the binding modes and the interactions are almost identical at the four binding

sites. These conformations are only marginally influenced by the slight rearrangement of external binding site residues as shown by the comparison of the four models. The interaction with the binding site is mainly hydrophobic, the unique exception being given by a possible H-bond between a nitrogen atom of the triazole core and the polar hydrogen of the amide function of Asn250 (TM6) residue. The presence of small substituents on the 2-phenyl ring modulates the interaction with TM5-6 residues, while small groups inserted at the 8-position provide an additional hydrophobic interaction with TM2-3 amino acids. A detailed view of the interaction of compound 7 (taken as template of Series C) with the hA3 AR model is depicted in Figure 3, Panels B and C. The presence of substituents at the 5-position (hence linked to the nitrogen atom of the quinoxaline ring) seems important but not critical for compound activity. The presence of small hydrophobic groups at this position improves the affinity for the receptor; this is not surprising and has already been shown even in the case of hA3AR agonists. 38–41 Binding data indicate that, on the whole, the propionyl group (COEt) (compounds 2, 7, 11) or the ethyl (COOEt, compounds 3, 9, 12) and methyl (COOMe, 5 and 8) carboxylate chain at the 5-position have a good effect on compound affinity. This is particularly true for derivatives bearing an 8-substituent, and can be considered true on the basis of the docking scores of the respective compounds. In the family 1 docking conformations, the phenyl group on the 5-substituent of compounds 14 and 15 is inserted between the hydrophobic side chains of Val169 (EL2) and Ile264 (TM7).

The second set of conformations (‘family 2’, Fig. 4, Panel A) is a mirror version of family 1, with analogue location of both the TQX scaffold and the 2-substituent, but with the fused phenyl ring pointing externally and located between Met174, Phe168, and Val169 (EL2), Ile249 and Ile253 (TM6), and Leu264 (TM7).

Just as for the family 1 conformations, the interaction with the binding site is mainly hydrophobic, the unique exception being a possible H-bond between a nitrogen atom of the triazole core and the polar hydrogen of the amide function of Asn250 (TM6) residue. The position and role of eventual small substituents on the 2-phenyl ring is analogous to family 1 conformations. Interestingly, the small groups, inserted at the 8-position and externally oriented, are located in analogous positions of the (small) 5-substituents in family 1 conformations. Conversely, the 5-substituents are positioned in an analogous position of 8-substituents in the case of family 1 conformations. Superimposition of the family 2 docking conformations of each compound on the four A3AR models shows that there are also some differences in compound orientation. The resulting family 2 conformations for compounds 14 and 15 present the tricyclic scaffold more externally oriented with the loss of Hbond interaction with Asn250. Moreover, the phenyl group on the 5-substituent of 14 and 15 could make the family 2 conformations for these two compounds difficult as there is not enough space to accommodate the 5-substituents in the subcavity between TM2 and TM3. This difficulty can be particularly evidenced for compound 15 that is endowed with reduced hA3 binding activity compared to most of the other N-5 substituted TQX derivatives. Thus, the lower affinity of this compound could be ascribed to its lower ability to assume both binding modes.

All together, the modeling results suggest that the compounds interact with the binding site through generally hydrophobic contact without the presence of strong H-bond or electrostatic interactions. On the other hand, the ability to present two reasonable ways of binding could be the key factor that leads to a higher affinity for the receptor. This result is particularly true for the compounds bearing the 8-substituent and small groups at N-5, for which the two docking conformations are almost equivalent from both the energy and score points of view. Compounds

24–27 seem able to assume both conformations as well, and the presence of the 8-substituent provides higher affinity (compare 24 and 26 to 25).

A docking analysis was performed also to simulate the possible binding modes of the simplified triazole derivatives 16–23 at the hA3AR binding site. The same docking and post-docking protocols were employed. Among these derivatives, only compound 23 showed nanomolar affinity at the hA3AR. The highest docking score conformation of this compound shows some similarities with family 1 conformations of tricyclic compounds described above. In particular, the triazole ring and the 3-aryl substituent of 23 are located in an analogous position of the triazole ring and the 2-substituent of the tricyclic derivatives 2–15, respectively. The 1-aryl ring mimics the role of the fused phenyl ring of the above described compounds, while the phenyl-urea function of 23 is externally oriented, with the phenyl ring inserted between Val169 (EL2) and Leu264 (TM7). An H-bond interaction occurs between the 4-nitrogen of triazole and a polar hydrogen atom of Asn250 (TM6) and we cannot exclude a possible second interaction involving a polar hydrogen atom of the compound urea function and the Asn250 carbonyl group. Among the monocyclic derivatives described in this work, compound 23 seems the only derivative able to fit the three subpockets of the hA3AR binding site indicated as I-III in Figure 5, Panel A, while the other simplified derivatives 16–19, lacking the side chain at the 5-position, do not seem able to properly interact with the binding site.

5. Conclusions

The present study has led to the identification of some 1,2,4-triazolo[1,5-a]quinoxalines as new hA3AR antagonists. In particular, the 5-substituted-4,5-dihydro derivatives 2–15 show, on the whole, good hA3 receptor affinity and in some cases selectivity versus all the other AR subtypes. Surprisingly, similar results are obtained with some TQX compounds (24–27), obtained as side

products, which lack all the classical structural requirements for anchoring at the hA3 receptor site, and maintain only the nude tricyclic scaffold. In contrast, the 1,2,4-triazole derivatives 16–23, designed as simplified structures from TQX compounds and preserving both the crucial NH and carbonyl groups and the two aryl moieties, turn out to be inactive or have very little activity at all the AR subtypes. The only exception is compound 23 which is endowed with micromolar hA3AR affinity and high selectivity versus both hA1 and hA2A subtypes. As a new finding, this triazole derivative emerges as lead candidate for the development of new monocyclic AR antagonists. On the whole, our results lead to new interesting insights about the structural requirements for hA3 receptor–ligand interaction. Molecular docking of tricyclic and simplified derivatives identify their hypothetical binding mode to our hA3 receptor model.

6. Experimental section

6.1. Chemistry

Silica gel plates (Merck F254) and silica gel 60 (Merck; 70–230 mesh) were used for analytical and column chromatography, respectively. All melting points were determined on a Gallenkamp melting point apparatus. Microanalyses were performed with a Flash E1112 Thermofinnigan elemental analyzer for C, H, N, and the results were within ±0.4% of the theoretical values except where stated otherwise. All final compounds revealed a purity not less than 95%. The IR spectra were recorded with a Perkin–Elmer Spectrum RX I spectrometer in Nujol mulls and are expressed in cm−1. The 1H NMR spectra were obtained with a Bruker Avance 400 MHz instrument. The chemical shifts are reported in δ (ppm) and are relative to the central peak of the solvent. The coupling constant (J) are expressed in Hz. All the exchangeable protons were confirmed by addition of D2O. The following abbreviations are used: s = singlet, d = doublet, dd = double doublet, t = triplet, m = multiplet, br = broad, ar = aromatic protons.

6.1.1. General procedure for the synthesis of 8-substituted 2-aryl-4,5-dihydro-1,2,4-triazolo[1,5-a]quinoxalines (32–35)26 and the corresponding 4,5-dehydro-derivatives (24–27)26

To a solution of the previously reported 2-aryl-4,5-dihydro-1,2,4-triazolo[1,5-a]quinoxalin-4-ones 28–3118, 26 (2.7 mmol) in anhydrous tetrahydrofuran (200 mL), heated at reflux under nitrogen atmosphere, an excess (21.5 mmol) of LiAlH4 was added portion by portion. At the end of the addition, the reaction mixture was maintained at reflux for 30 min. Then ice (200 g) was carefully added and the mixture was kept under stirring until gas evolution ended. The aqueous phase was extracted with ethyl acetate (100 mL × 2), and the separated organic layers were washed with water (60 mL × 2), anhydrified (Na2SO4) and evaporated under reduced pressure. The crude mixture, composed by the 4,5-dihydro-derivatives 32–35 and the corresponding dehydro-compounds 24–27, was separated by silica gel column chromatography, eluting system chloroform/methanol 9.5:0.5 (24 and 32), chloroform/methanol 9:1 (25 and 33), chloroform/acetone 8:2 (26 and 34), dichloromethane/cyclohexane/ethyl acetate 9:0.5:0.5 (27 and 35).

6.1.1.1. 8-Chloro-2-phenyl-4,5-dihydro-1,2,4-triazolo[1,5-a]quinoxaline (32)

Yield: 24%; mp 176–178 °C dec (ethanol). 1H NMR (DMSO-d6) δ: 4.78 (s, 2H, CH2), 6.74 (s, 1H, NH), 6.85 (d, 1H, ar J = 8.79), 7.12 (d, 1H, ar, J = 8.06), 7.49–7.58 (m, 4H, ar), 8.08–8.10 (m, 2H, ar). IR: 3295. Anal. Calcd for (C15H11ClN4): C, 63.72; H, 3.92; N 19.82; Found: C, 62.99; H, 3.41; N, 19.98.

6.1.1.2. 2-Phenyl-4,5-dihydro-1,2,4-triazolo[1,5-a]quinoxaline (33)

Yield: 30%; mp 126–128 °C (ethyl acetate) (lit. mp 126–128 °C).26

6.1.1.3. 8-Methyl-2-phenyl-4,5-dihydro-1,2,4-triazolo[1,5-a]quinoxaline (34)

Yield: 37%; mp 177–179 °C (ethanol). 1H NMR (DMSO-d6) δ: 2.26 (s, 3H, CH3), 4.68 (s, 2H, CH2), 6.36 (s, 1H, NH), 6.75 (d, 1H, ar, J = 8,06), 6.88 (d, 1H, ar, J = 8.06), 7.44–7.54 (m, 4H, ar), 8.05–8.10 (m, 2H, ar). IR 3300. Anal. Calcd for (C16H14N4): C, 73.26; H, 5.38; N 21.36; Found: C, 73.58; H, 4.71; N, 20.87.

6.1.1.4. 2-(4-Methoxyphenyl)-8-methyl-4,5-dihydro-1,2,4-triazolo[1,5-a]quinoxaline (35)

Yield: 35% (impure); 1H NMR (DMSO-d6) δ: 2.27 (s, 3H, CH3), 3.83 (s, 3H, OCH3), 4.67 (s, 2H, CH2), 6.32 (s, 1H, NH), 6.75 (d, 1H, ar, J = 8.19), 6.89 (d, 1H, ar, J = 8.17 Hz), 7.06 (d, 2H, ar, J = 8.53), 7.43 (s, 1H, ar), 8.01 (d, 2H, ar, J = 8.57). Anal. Calcd for (C17H16N4O): C, 69.85; H, 5.52; N 19.17; Found: C, 70.12; H, 5.75; N, 19.32.

6.1.1.5. 8-Chloro-2-phenyl-1,2,4-triazolo[1,5-a]quinoxaline (24)

Yield: 24%; mp 217–219 °C (ethyl acetate). 1H NMR (DMSO-d6) δ: 7.58–7.61 (m, 3H, ar), 7.86 (dd, 1H, ar, J = 8.79, 2.2), 8.25–8.35 (m, 3H, ar), 8.52 (d, 1H, ar, J = 2.2), 9.51 (s, 1H, ar). IR: 1090, 820. Anal. Calcd for (C15H9ClN4): C, 64.18; H, 3.23; N 19.96; Found: C, 64.86; H, 3.74; N, 20.13.

6.1.1.6. 2-Phenyl-1,2,4-triazolo[1,5-a]quinoxaline (25)

Yield: 5%; mp 174–176 °C (ethanol) (lit. mp 181–183 °C).26

6.1.1.7. 8-Methyl-2-phenyl-1,2,4-triazolo[1,5-a]quinoxaline (26)

Yield: 10%; mp 162–164 °C (ethanol). 1H NMR (DMSO-d6) δ: 2.64 (s, 3H, CH3), 7.58–7.66 (m, 4H, ar), 8.13 (d, 1H, ar, J = 8.06), 8.29–8.32 (m, 3H, ar), 9.40 (s, 1H, ar). Anal. Calcd for (C16H12N4): C, 73.83; H, 4.65; N 21.52; Found: C, 74.23; H, 4.05; N, 20.97.

6.1.1.8. 2-(4-Methoxyphenyl)-8-methyl-1,2,4-triazolo[1,5-a]quinoxaline (27)

Yield: 30%; mp 180–182 °C (cyclohexane). 1H NMR (DMSO-d6) δ: 2.65 (s, 3H, CH3), 3.87 (s, 3H, OCH3), 7.16 (d, 2H, ar, J = 8.59), 7.64 (d, 1H, ar, J = 8.16), 8.13 (d, 1H, ar, J = 8.24), 8.25 (d, 2H, ar, J = 8.56), 8.32 (s, 1H, ar), 9.38 (s, 1H, CH). Anal. Calcd for (C17H14N4O): C, 70.33; H, 4.86; N 19.30; Found: C, 69.76; H, 5.01; N, 19.12.

6.1.2. Synthesis of 2-Phenyl-1,2,4-triazolo[1,5-a]quinoxalines (25, 27)

A mixture of compounds 25, 33 or 27, 35 (0.2 g) in glacial acetic acid (5 mL) was heated at reflux for 5 h. Evaporation of the solvent at reduced pressure to small volume produced separation of a solid which was collected and washed with diethyl ether.

2-Phenyl-1,2,4-triazolo[1,5-a]quinoxaline (25).26 Yield: 26%.

2-(4-Methoxyphenyl)-8-methyl-1,2,4-triazolo[1,5-a]quinoxaline (27). Yield: 30%.

6.1.3. General procedure for the synthesis of N-5-substituted 2-aryl-4,5-dihydro-1,2,4-triazolo[1,5-a]quinoxaline derivatives (2–15)

To a suspension of compounds 32–3526 (1.2 mmol) and small amounts of the corresponding 4,5-dehydro-derivatives 24–27 in anhydrous dichloromethane (40 mL) and anhydrous pyridine (0.1 mL) kept at 0 °C and under nitrogen atmosphere, a solution of the suitable acyl chloride or chloroformates (3.6 mmol) in anhydrous dichloromethane (4.0 mL) was drop by drop added. The reaction was stirred at 0 °C for 30 min (compounds 11–15), at room temperature for 1 h (4–5, 7,

9–10), 4 h (compound 8), otherwise at reflux for 3 h (2–3, 6). After evaporation of the solvent at reduced pressure, the crude mixture was purified by silica gel column chromatography by using the suitable eluting system.

6.1.3.1. 1-(8-Chloro-2-phenyl-1,2,4-triazolo[1,5-a]quinoxalin-5(4H)-yl)-propan-1-one (2)

Eluting system: chloroform/methanol 9.9:0.1. Yield: 25%; mp 142–144 °C (cyclohexane). 1H NMR (DMSO-d6) δ: 0.99 (t, 3H, CH3, J = 7.33), 2.58 (q, 2H, CH2, J = 7.33), 5.24 (s, 2H, CH2), 7.43–7.53 (m, 4H, ar), 7.79–7.83 (m, 2H, ar), 8.09–8.13 (m, 2H, ar). IR: 1680. Anal. Calcd for (C18H15ClN4O) C, 63.81; H, 4.46; N 16.54; Found: C, 63.24; H, 4.15; N, 17.02.

6.1.3.2. Ethyl 8-chloro-2-phenyl-1,2,4-triazolo[1,5-a]quinoxalin-5(4H)-carboxylate (3)

Eluting system: chloroform/methanol 9.9:0.1. Yield: 48%; mp 177–179 °C (ethanol). 1H NMR (DMSO-d6) δ: 1.26 (t, 3H, CH3, J = 6.96), 4.22 (q, 2H, CH2, J = 6.96), 5.21 (s, 2H, CH2), 7.42–7.58 (m, 4H, ar), 7.80–7.84 (m, 2H, ar), 8.07–8.13 (m, 2H, ar). IR: 1715. Anal. Calcd for (C18H15ClN4O2): C, 60.94; H, 4.26; N 15.79; Found: C, 61.78; H, 4.18; N, 16.06.

6.1.3.3. 1-(2-Phenyl-1,2,4-triazolo[1,5-a]quinoxalin-5(4H)-yl)-propan-1-one (4)

Eluting system: cyclohexane/ethyl acetate/methanol 6:3.5:0.5. Yield: 28%; mp 126–128 °C (ethanol). 1H NMR (DMSO-d6) δ: 1.06 (t, 3H, CH3, J = 7.29), 2.58 (q, 2H, CH2, J = 7.29), 5.25 (s, 2H, CH2), 7.40–7.53 (m, 5H, ar), 7.77 (d, 1H, ar, J = 6.73), 7.87 (d, 1H, ar, J = 7.40), 8.11 (d, 2H, ar, J = 6.73). IR: 1680. Anal. Calcd for (C18H16N4O): C, 71.04; H, 5.30; N 18.41; Found: C, 71.37; H, 4.83; N, 18.07.

6.1.3.4. Methyl 2-phenyl-1,2,4-triazolo[1,5-a]quinoxalin-5(4H)-carboxylate (5)

Eluting system: cyclohexane/ethyl acetate/methanol 8:3:0.15. Yield: 21%; mp 149–151 °C (methanol). 1H NMR (DMSO-d6) δ: 3.77 (s, 3H, OCH3), 5.22 (s, 2H, CH2), 7.40–7.47 (m, 2H, ar), 7.49–7.54 (m, 3H, ar), 7.79 (d, 1H, ar, J = 8.51), 7.86 (d, 1H, ar, J = 6.73), 8.11 (d, 2H, ar, J = 6.73). IR: 1700. Anal. Calcd for (C17H14N4O2): C, 66.66; H, 4.61; N 18.29; Found: C, 65.98; H, 4.33; N, 18.71.

6.1.3.5. Ethyl 2-phenyl-1,2,4-triazolo[1,5-a]quinoxalin-5(4H)-carboxylate (6)

Eluting system: dichloromethane/methanol 9.8:0.2. Yield: 38%; mp 116–118 °C (methanol). 1H NMR (DMSO-d6) δ: 1.27 (t, 3H, CH3, J = 6.96), 4.23 (q, 2H, CH2, J = 6.96), 5.22 (s, 2H, CH2), 7.40–7.47 (m, 2H, ar), 7.49–7.54 (m, 3H, ar), 7.80 (d, 1H, ar, J = 6.73), 7.85 (d, 1H, ar, J = 4.94), 8.11 (d, 2H, ar, J = 6.73). IR 1700. Anal. Calcd for (C18H16N4O2): C, 67.49; H, 5.03; N 17.49; Found: C, 68.93; H, 4.71; N, 17.94.

6.1.3.6. 1-(8-Methyl-2-phenyl-1,2,4-triazolo[1,5-a]quinoxalin-5(4H)-yl)-propan-1-one (7)

Eluting system: chloroform/acetone 9:1. Yield 31%; mp 150–152 °C (cyclohexane). 1H NMR (DMSO-d6) δ: 0.98 (t, 3H, CH3, J = 6.96), 2.43–2.57 (m, 5H, CH2+CH3), 5.21 (s, 2H, CH2), 7.20 (d, 1H, ar, J = 8.06), 7.49–7.52 (m, 3H, ar), 7.61–7.690(m, 2H, ar), 8.08–8.12 (m, 2H, ar). IR: 1670. Anal. Calcd for (C19H18N4O): C, 71.68; H, 5.70; N 17.60; Found: C, 70.85; H, 5.51; N, 18.10.

6.1.3.7. Methyl 8-methyl-2-phenyl-1,2,4-triazolo[1,5-a]quinoxalin-5(4H)-carboxylate (8)

Eluting system: dichloromethane/methanol 9.8:0.2. Yield: 12%; mp 132–134 °C (methanol). 1H NMR (DMSO-d6) δ: 2.40 (s, 3H, CH3), 3.74 (s, 3H, OCH3), 5.17 (s, 2H, CH2), 7.18 (d, 1H, ar,

J = 8.06), 7.49–7.52 (m, 3H, ar), 7.61–7.66 (m, 2H, ar), 8.07–8.11 (m, 2H, ar). IR: 1720. Anal. Calcd for (C18H16N4O2): C, 67.49; H, 5.03; N 17.49; Found: C, 68.15; H, 4.67; N, 17.95.

6.1.3.8. Ethyl 8-methyl-2-phenyl-1,2,4-triazolo[1,5-a]quinoxalin-5(4H)-carboxylate (9)

Eluting system: dichloromethane/acetone/cyclohexane 8.8:0.7:0.5. Yield: 56%; mp 176–178 °C (ethyl acetate). 1H NMR (DMSO-d6) δ: 1.25 (t, 3H, CH3, J = 6.96), 2.41 (s, 3H, CH3), 4.19 (q, 2H, CH2, J = 6.96), 5.18 (s, 2H, CH2N), 7.19 (d, 1H, ar, J = 8.79), 7.50–7.53 (m, 3H, ar), 7.63–7.68 (m, 2H, ar), 8.08–8.12 (m, 2H, ar). IR: 1715. Anal. Calcd for (C19H18N4O2): C, 68.25; H, 5.43; N 16.76; Found: C, 68.77; H, 4.66; N, 16.12.

6.1.3.9. n-Propyl 8-methyl-2-phenyl-1,2,4-triazolo[1,5-a]quinoxalin-5(4H)-carboxylate (10)

Eluting system: chloroform. Yield: 70%; mp 117–119 °C (ethanol). 1H NMR (DMSO-d6) δ: 0.90 (t, 3H, CH3, J = 7.41), 1.58–1.69 (m, 2H, CH2), 2.40 (s, 3H, CH3), 4.10 (t, 2H, CH2O, J = 6.23), 5.17 (s, 2H, CH2N), 7.18 (d, 1H, ar, J = 8.42), 7.49–7.58 (m, 3H, ar), 7.62–7.66 (m, 2H, ar), 8.08–8.10 (m, 2H, ar). IR: 3070, 1725. Anal. Calcd for (C20H20N4O2): C, 68.95; H, 5.79; N 16.08; Found: C, 69.56; H, 5.47; N, 16.27.

6.1.3.10. 1-[2-(4-Methoxyphenyl)-8-methyl-1,2,4-triazolo[1,5-a]quinoxalin-5(4H)-yl]-propan-1-one (11)

Eluting system: cyclohexane/ethyl acetate/methanol 9:2:1. Yield: 21%; mp 132–133 °C (cyclohexane); 1H NMR (DMSO-d6) δ: 1.00 (t, 3H, CH3, J = 6.64), 2.44–2.53 (m, 5H, CH2+CH3), 3.83 (s, 3H, OCH3), 5.20 (s, 2H, CH2N), 7.08 (d, 2H, ar, J = 8.52), 7.20 (d, 1H, ar, J = 8.32), 7.63 (d, 1H, ar, J = 7.60), 7.68 (s, 1H, ar), 8.03 (d, 2H, ar, J = 8.52). Anal. Calcd for (C20H20N4O2): C, 68.95; H, 5.79; N 16.08; Found: C, 68.13; H, 5.99; N, 15.83.

6.1.3.11. Ethyl 2-(4-methoxyphenyl)-8-methyl-1,2,4-triazolo[1,5-a]quinoxalin-5(4H)-carboxylate (12)

Eluting system: dichloromethane/cyclohexane/ethylacetate 9:0.5:0.5. Yield: 21%; mp 141–142 °C (cyclohexane); 1H NMR (DMSO-d6) δ: 1.26 (t, 3H, CH3, J = 7.08), 2.42 (s, 3H, CH3), 3.84 (s, 3H, OCH3), 4.19 (q, 2H, CH2, J = 7.08), 5.17 (s, 2H, CH2), 7.08 (d, 2H, ar, J = 8.76), 7.19 (d, 1H, ar, J = 8.40), 7.65–7.67 (m, 2H, ar), 8.03 (d, 2H, ar, J = 8.76). IR: 1708. Anal. Calcd for (C20H20N4O3): C, 65.92; H, 5.53; N 15.38; Found: C, 66.66; H, 5.78; N, 14.87.

6.1.3.12. Propyn-2-yl 2-(4-methoxyphenyl)-8-methyl-1,2,4-triazolo[1,5-a]quinoxalin-5(4H)-carboxylate (13)

Eluting system: cyclohexane/ethyl acetate 6:4. Yield 21%. mp 134–135 °C (cyclohexane); 1H NMR (DMSO-d6) δ: 2.42 (s, 3H, CH3), 3.63 (s, 1H, CCH), 3.84 (s, 3H, OCH3), 4.84 (s, 2H, OCH2), 5.18 (s, 2H, NCH2), 7.09 (d, 2H, ar, J = 8.40), 7.21 (d, 1H, ar, J = 7.68), 7.62 (d, 1H, ar, J = 7.68), 7.68 (s, 1H, ar), 8.04 (d, 2H, ar, J = 8.48). IR: 3260, 1721. Anal. Calcd for (C21H18N4O3): C, 67.37; H, 4.85; N 14.96; Found: C, 67.97; H, 4.05; N, 15.13.

6.1.3.13. 2-Phenyl-1-[2-(4-methoxyphenyl)-8-methyl-1,2,4-triazolo[1,5-a]quinoxalin-5(4H)-yl)-ethanone (14)

Eluting system: dichloromethane/acetone 9:1. Yield: 22%; mp 188–190 °C (cyclohexane); 1H NMR (DMSO-d6) δ: 2.44 (s, 3H, CH3), 3.84 (s, 3H, OCH3), 3.96 (s, 2H, COCH2), 5.22 (s, 2H, CH2N), 7.08 (d, 2H, ar, J = 7.12), 7.10–7.23 (m, 6H, ar), 7.66–7.70 (m, 2H, ar), 8.03 (d, 2H, ar, J = 7.12). IR: 1662. Anal. Calcd for (C25H22N4O2): C, 73.15; H, 5.40; N 13.65; Found: C, 72.54; H, 5.63; N, 14.15.

6.1.3.14. Benzyl 2-(4-methoxyphenyl)-8-methyl-1,2,4-triazolo[1,5-a]quinoxalin-5(4H)-carboxylate (15)

Eluting system: cyclohexane/ethyl acetate 6:4. Yield: 31%, mp 119–120 °C (cyclohexane); 1H NMR (DMSO-d6) δ: 2.40 (s, 3H, CH3), 3.83 (s, 3H, OCH3), 5.19 (s, 2H, OCH2), 5.23 (s, 2H, NCH2), 7.10 (d, 2H, ar, J = 8.61), 7.17 (d, 1H, ar, J = 8.24), 7.35–7.45 (m, 5H, ar), 7.66 (m, 2H, ar), 8.03 (d, 2H, ar, J = 8.60). IR: 1722. Anal. Calcd for (C25H22N4O3): C, 70.41; H, 5.20; N 13.14; Found: C, 70.59; H, 4.66; N, 13.91.

6.1.4. 3-(4-Methoxyphenyl)-1-(5-methyl-2-nitrophenyl)-1,2,4-triazole-5-chloromethyl (37)

To a solution of chloroacetyl chloride (3.4 mmol) in anhydrous toluene (15 mL) at 80 °C, the amidrazone 3618 (1.7 mmol) was added portion by portion. The reaction mixture was heated at reflux for 3 h. Then, the solvent was removed under reduced pressure and the oily residue was worked up with a mixture of ethyl acetate/petroleum ether 1:1. The solid which separated was collected by filtration and washed with petroleum ether. Yield: 72%; mp 127–128 °C (ethanol); 1H NMR (DMSO-d6) δ: 2.51 (s, 3H, CH3), 3.82 (s, 3H, OCH3), 4.95 (s, 2H, CH2), 7.07 (d, 2H, ar, J = 8.88), 7.72 (d, 1H, ar, J = 8.32), 7.81(s, 1H, ar), 7.93 (d, 2H, ar, J = 8.88), 8.23 (d, 1H, ar, J = 8.40). Anal. Calcd for (C17H15Cl N4O3): C, 56.91; H, 4.21; N 15.66; Found: C, 57.27; H, 4.10; N, 16.09.

6.1.5. 2-(4-Methoxyphenyl)-8-methyl-4,5-dihydro-1,2,4-triazolo[1,5-a]quinoxaline (35)

To a solution of the 5-chloromethyl-1,2,4-triazole derivative 37 (1.59 mmol) in ethanol (75 mL), an excess of SnCl2 dihydrate (4.77 mmol) was added under nitrogen atmosphere. Then, the reaction mixture was heated at reflux, under nitrogen atmosphere, for 40 h. After evaporation of

the solvent at reduced pressure, the resulting solid was worked up with diethyl ether, collected by filtration and washed with a large amount of water. The crude product, containing a small amount of the dehydro-derivative 27 (27/35, ratio 1:10, 1H NMR evaluation) was used as it is for the next step. Yield: 83%.

6.1.6. 3-(4-Methoxyphenyl)-1-(5-methyl-2-nitrophenyl)-1,2,4-triazole (38)

To a suspension of the amidrazone 3618 (1.0 mmol) in ethyl orthoformate (1.25 mL), p-toluenesulfonic acid (10 mg) was added. The reaction mixture was heated at 100 °C for 30 min. Upon cooling, a orange solid precipitated which was collected by filtration and washed with diethyl ether. Yield 54%; mp 138–139 °C (ethanol); 1H NMR (DMSO-d6) δ: 2.50 (s, 3H, CH3), 3.82 (s, 3H, OCH3), 7.06 (d, 2H, ar, J = 8.76), 7.60 (d, 1H, ar, J = 8.36), 7.80 (s, 1H, ar), 7.94 (d, 2H, ar, J = 8.70), 8.09 (d, 1H, ar, J = 8.36), 9.09 (s, 1H, CH). Anal. Calcd for (C16H14N4O3): C, 61.93; H, 4.55; N 18.06; Found: C, 61.13; H, 4.89; N, 18.72.

6.1.7. 2-[3-(4-Methoxyphenyl)-1,2,4-triazol-1-yl]-4-methyl-phenylamine (39)

To a solution of the 2-nitrophenyl-1,2,4-triazole derivative 38 (2.0 mmol) in ethyl acetate (50 mL), the catalyst (10% Pd/C, 50 mg) was added. Hydrogenation of the resulting mixture was performed at 30 Psi until disappearance of the starting material (TLC monitoring, eluting system cyclohexane/ethyl acetate 6:4). The catalyst was removed by filtration and the solvent was distilled under reduced pressure to yield a solid. Yield 69%; mp 131–132 °C (ethanol); 1H NMR (DMSO-d6) δ: 2.22 (s, 3H, CH3), 3.82 (s, 3H, OCH3), 5.31 (s, 2H, NH2), 6.84 (d, 1H, ar, J = 8.24), 7.02 (d, 1H, ar, J = 8.20), 7.06 (d, 2H, ar, J = 8.80), 7.14 (s, 1H, ar), 8.02 (d, 2H, ar, J = 8.76), 8.83 (s, 1H, CH). IR: 3448, 3348 Anal. Calcd for (C16H16N4O): C, 68.55; H, 5.75; N 19.99; Found: C, 67.71; H, 5.05; N, 20.17.

6.1.8. General procedure for the synthesis of 2-[3-(4-methoxyphenyl)-1,2,4-triazol-1-yl]-4-methyl-phenylcarbamates (16–19)

A solution of the suitable chloroformates (compounds 16–17, 19) (3.2 mmol) or phenacetyl chloride (18) (3.2 mmol) in anhydrous dichloromethane (3.2 mL) was drop by drop added to a solution of the triazole derivative 39 (1.07 mmol) in anhydrous dichloromethane (32 mL) and anhydrous pyridine (0.05 mL) at 0 °C. The reaction mixture was kept at 0 °C for 2 h. Then, the solvent was removed under reduced pressure and the solid was worked up with water (20 mL), collected and washed with water (compounds 16–17, 19). Otherwise (compound 18), the solid was worked up with 10% aqueous solution of NaHCO3 (20 mL), and the resulting mixture extracted with ethyl acetate (15 mL × 3). The organic layers were washed with water (20 mL), anhydrified (Na2SO4) and evaporated under reduced pressure to give a yellow solid.

6.1.8.1. Ethyl 2-[3-(4-methoxyphenyl)-1H-1,2,4-triazol-1-yl]-4-methylphenylcarbamate (16)

Yield: 85%; mp 117–118 °C (cyclohexane); 1H NMR (DMSO-d6) δ: 1.12 (t, 3H, CH3, J = 7.08), 2.37 (s, 3H, CH3), 3.83 (s, 3H, OCH3), 4.03 (q, 2H, CH2, J = 7.08), 7.07 (d, 2H, ar, J = 8.88), 7.30 (d, 1H, ar, J = 8.41), 7.45 (s, 1H, ar), 7.58 (d, 1H, ar, J = 8.16), 8.00 (d, 2H, ar, J = 8.84), 8.84 (s, 1H, CH), 9.13 (s, 1H, NH). IR: 1726. Anal. Calcd for. (C19H20N4O3): C, 64.76; H, 5.72; N 15.90; Found: C, 64.66; H, 5.01; N, 16.18.

6.1.8.2. Propyn-2-yl 2-[3-(4-methoxyphenyl)-1H-1,2,4-triazol-1-yl]-4-methylphenylcarbamate (17)

Yield: 54%; mp 132–133 °C (cyclohexane); 1H NMR (DMSO-d6) δ: 2.37 (s, 3H, CH3), 3.53 (s, 1H, CH), 3.83 (s, 3H, OCH3), 4.68 (s, 2H, CH2), 7.07 (d, 2H, ar, J = 8.88), 7.32 (d, 1H, ar, J =

8.28), 7.46 (s, 1H, ar), 7.59 (d, 1H, ar, J = 8.04), 8.01 (d, 2H, ar, J = 8.90), 8.84 (s, 1H, CH), 9.37 (s, 1H, NH). IR: 1720. Anal. Calcd for (C20H18N4O3): C, 66.29; H, 5.01; N 15.46; Found: C, 66.76; H, 4.55; N, 14.93.

6.1.8.3. N-[2-(3-(4-methoxyphenyl)-1H-1,2,4-triazol-1-yl)-4-methylphenyl]-2-phenylacetamide (18)

Yield: 76%; mp 138–139 °C (ethanol); 1H NMR (DMSO-d6) δ: 2.36 (s, 3H, CH3), 3.59 (s, 2H, CH2), 3.84 (s, 3H, OCH3), 7.09 (d, 2H, ar, J = 8.80), 7.19 (s, 5H, ar), 7.30 (d, 1H, ar, J = 8.44), 7.43 (s, 1H, ar), 7.71 (d, 1H, ar, J = 8.32), 8.01 (d, 2H, ar, J = 8.80), 8.50 (s, 1H, CH), 9.72 (s, 1H, NH). IR: 3247, 3096, 1688. Anal. Calcd for (C24H22N4O2): C, 72.34; H, 5.57; N 14.06; Found: C, 73.05; H, 5.74; N, 14.54.

6.1.8.4. Benzyl 2-[3-(4-methoxyphenyl)-1H-1,2,4-triazol-1-yl]-4-methylphenylcarbamate (19)

Yield: 34%; mp 149–150 °C (ethanol); 1H NMR (DMSO-d6) δ: 2.37 (s, 3H, CH3), 3.83 (s, 3H, OCH3), 5.06 (s, 2H, CH2), 7.06 (d, 2H, ar, J = 8.68), 7.31 (s, 6H, ar), 7.46 (s, 1H, ar), 7.61 (d, 1H, ar, J = 8.08), 8.00 (d, 2H, ar, J = 8.61), 8.85 (s, 1H, CH), 9.34 (s, 1H, NH). IR: 3227, 3109, 1728. Anal. Calcd for (C24H22N4O3): C, 69.55; H, 5.35; N 13.52; Found: C, 68.88; H, 4.95; N, 14.18.

6.1.9. N1-Phenyl-N2-(4-methoxybenzoyl)-hydrazide (40)[27,28]

To a mixture of phenylhydrazine (9.25 mmol) in anhydrous pyridine (10 mL) a solution of equimolar amount of p-anisoyl chloride in anhydrous pyridine (5 mL) was drop by drop added. The reaction mixture was heated at reflux for 5 h. The excess of pyridine was removed by

distillation under reduced pressure. The residue was treated with HCl 2 M solution (30 mL) and the resulting solid was collected by filtration and well washed with water. Yield: 75%; mp 165–168 °C (ethanol) (lit. Mp 177–178 °C).28

6.1.10. N1-Phenyl-N2-[α-chloro-(4-methoxybenzyliden)]hydrazine (41)29

A suspension of equimolar amount of hydrazide 4027, 28 (4.13 mmol) and PCl5 in POCl3 (7 mL) was heated at reflux for 4 h. Then, another portion (4.13 mmol) of PCl5 was added and the heating continued for 2 h. Evaporation at reduced pressure of the excess of POCl3 gave an oily residue which was treated with cold water (50 mL) and quickly collected. The compound was used as it is without further purification. Yield: 90%; mp 117–121 °C (lit. mp 119–120 °C). 1H NMR (CDCl3) δ: 3.89 (s, 3H, OCH3), 6.98 (d, 2H, ar, J = 8.60), 7.33–7.35 (m, 1H, ar), 7.38–7.46 (m, 4H, ar), 8.06 (d, 2H, ar, J = 8.61).

6.1.11. 3-(4-Methoxyphenyl)-1-phenyl-1H-1,2,4-triazol-5-amine (42)

A mixture of the chloro-derivative 4129 (4.12 mmol) and an excess of cyanamide (20.6 mmol) was heated at 100 °C for 20 min. The crude mass was worked up with ethyl acetate (20 mL) and the resulting solid was filtered off and well washed with ethyl acetate. The mother liquors were evaporated under reduced pressure to yield a solid which was purified by silica gel column chromatography, eluting system: dichloromethane/methanol 9:1, and then dichloromethane/ethyl acetate 8:2. Yield: 45%; mp 152–155 °C (toluene). 1H NMR (DMSO-d6) δ: 3.80 (s, 3H, OCH3), 6.51 (br s, 2H, NH2), 7.01 (d, 2H, ar, J = 8.68), 7.39 (t, 1H, ar, J = 7.28), 7.54 (t, 2H, ar, J = 7.64), 7.62 (d, 2H, ar, J = 7.88), 7.88 (d, 2H, ar, J = 8.60). IR: 3303. Anal. Calcd for (C15H14N4O): C, 67.65; H, 5.30; N 21.04; Found: C, 67.93; H, 4.87; N, 21.27.

6.1.12. N-Acetyl-N-[3-(4-methoxyphenyl)-1-phenyl-1H-1,2,4-triazol-5-yl]acetamide (20)

A mixture of the triazole 42 (0.75 mmol) and acetic anhydride (2.25 mmol) in anhydrous pyridine (3 mL) was heated at reflux for 8 h. The crude mass was worked up with water and the resulting solid collected by filtration ad purified by silica gel column chromatography, eluting system dichloromethane/ethyl acetate 8:2. Yield: 38%; mp 130–132 °C (cyclohexane/ethyl acetate 8:2); 1H NMR (DMSO-d6) δ: 2.29 (2, 6H, 2CH3), 3.83 (s, 3H, OCH3), 7.09 (d, 2H, ar, J = 8.64), 7.54–7.60 (m, 5H, ar), 8.01 (d, 2H, ar, J = 8.64). IR: 1749, 1715. Anal. Calcd for (C19H18N4O3): C, 65.13; H, 5.18; N 15.99; Found: C, 64.66; H, 5.45; N, 16.35.

6.1.13. General procedure for the synthesis of N-[3-(4-methoxyphenyl)1-phenyl-1H-1,2,4-triazol-5-yl]benzamide (21) and N-benzoyl-N-[3-(4-methoxyphenyl)-1-phenyl-1H-1,2,4-triazol-5-yl]benzamide (22)

A solution of a little excess of benzoyl chloride (0.54 mmol) in anhydrous tetrahydrofuran (2 mL) was drop by drop added to a solution of the 1,2,4-triazol-5-amino derivative 42 (0.45 mmol) in anhydrous tetrahydrofuran (8 mL) and anhydrous pyridine (3 mL). The reaction mixture was heated at reflux for 25 h. After 10 h, another portion (0.5 mmol) of benzoyl chloride was added. After cooling, water (30 mL) and ice (20 g) were added and the resulting solution was extracted with ethyl acetate (30 mL × 4). The organic layers were washed with water (30 mL × 4), with a saturated solution of NaHCO3 (30 mL), and again with water (40 mL), then anhydrified (Na2SO4) and evaporated under reduced pressure. The resulting oily residue was purified by silica gel column chromatography, eluting system dichloromethane/ethyl acetate 1:1.

6.1.13.1. Compound (21)

Yield: 20%; mp 156–158 °C (diethyl ether/petroleum ether); 1H NMR (DMSO-d6) δ: 3.84 (s, 3H, OCH3), 7.08 (d, 2H, ar, J = 8.44), 7.42 (t, 1H, ar, J = 6.88), 7.50–7.56 (m, 4H, ar), 7.65 (d, 3H, ar, J = 7.16), 7.91 (d, 2H, ar, J = 7.40), 8.01 (d, 2H, ar, J = 8.36), 11.17 (s, br, 1H, NH). IR: 3194, 1667. Anal. Calcd for (C22H18N4O2): C, 71.34; H, 4.90; N 15.13; Found: C, 70.67; H, 5.30; N, 14.59.

6.1.13.2. Compound (22)

Yield: 60%; mp 154–156 °C (ethanol); 1H NMR (DMSO-d6) δ: 3.82 (s, 3H, OCH3), 7.05 (d, 2H, ar, J = 6.88), 7.41–7.45 (m, 6H, ar), 7.50–7.55 (m, 3H, ar), 7.59 (t, 2H, ar, J = 7.48), 7.63 (d, 4H, ar, J = 7.12), 7.93 (d, 2H, ar, J = 4.88). IR: 1708. Anal. Calcd for. (C29H22N4O3): C, 73.40; H, 4.67; N 11.81; Found: C, 73.01; H, 5.10; N, 11.12.

6.1.14. 1-[3-(4-Methoxyphenyl)-1-phenyl-1H-1,2,4-triazol-5-yl]-3-phenylurea (23)

A solution of phenylisocyanate (0.26 mmol) in anhydrous dichloromethane (4 mL) was drop by drop added to an equimolar amount of the 5-aminotriazole 42 in anhydrous dichloromethane (4 mL) maintained at 5 °C. The reaction mixture was then kept at room temperature for 20 days. The solvent was removed until small volume and the resulting solid was collected. Yield 42%; mp 202–204 °C (2-methoxyethanol); 1H NMR (DMSO-d6) δ: 3.83 (s, 3H, OCH3), 7.02 (t, 1H, ar, J = 7.20), 7.07 (d, 2H, ar, J = 8.44), 7.30 (t, 2H, ar, J = 7.25), 7.44–7.49 (m, 3H, ar), 7.57 (t, 2H, ar, J = 7.44), 7.66 (d, 2H, ar, J = 7.84), 7.99 (d, 2H, ar, J = 8.32), 9.43 (s, 1H, NH), 9.75 (s, 1H, NH). IR: 3182, 3145, 1685. Anal. Calcd for (C22H19N5O2): C, 68.56; H, 4.97; N 18.17; Found: C, 69.07; H, 5.31; N, 18.44.

6.2. Computational methodologies

All molecular modeling studies were performed on a 2 CPU (PIV 2.0–3.0 GHZ) Linux PC. Homology modeling, energy minimization, and docking studies were carried out using Molecular Operating Environment (MOE, version 2010.10) suite.35 Manual docking and Monte Carlo studies of the MRS 1220 binding mode were done using MOE and Schrodinger Macromodel (ver. 8.0)42 with Schrodinger Maestro interface. Compounds docking analyses were then performed with MOE. All ligand structures were optimized using RHF/AM1 semiempirical calculations and the software package MOPAC implemented in MOE was utilized for these calculations.37

6.2.1. Homology modeling of the human A3AR

Homology models of the hA3AR were built using recently solved X-ray structures of the antagonist-bound hA2A AR as templates (pdb code: 3EML; 2.6-Å resolution;30 pdb code: 3PWH; 3.3-Å resolution;31 pdb code: 3REY; 3.3-Å resolution;31 pdb code: 3UZA; 3.3-Å resolution32). A multiple alignment of the AR primary sequences was built within MOE as preliminary step. For all hA3AR models, the boundaries identified from the used X-ray crystal structure of hA2A AR were then applied for the corresponding sequences of the TM helices of the hA3AR. The missing loop domains were built by the loop search method implemented in MOE. Once the heavy atoms were modeled, all hydrogen atoms were added, and the protein coordinates were then minimized with MOE using the AMBER99 force field.43 The minimizations were performed by 1000 steps of steepest descent followed by conjugate gradient minimization until the RMS gradient of the potential energy was less than 0.05 kJ mol−1 Å−1. The reliability and quality of these models were checked using the Protein Geometry Monitor application within MOE, which provides a variety of stereochemical measurements for inspection of the structural quality in a given protein, like backbone bond lengths, angles and

dihedrals, Ramachandran φ–ψ dihedral plots, and sidechain rotamer and non-bonded contact quality.

6.2.2. Preliminary docking analysis with MRS 1220

A preliminary docking analysis was performed by manually docking MRS 1220 structure within each hA3AR model binding site. The obtained hA3AR–MRS 1220 complexes were then subjected to energy minimization refinement and to Monte Carlo analysis to explore the favorable binding conformations. This analysis was conducted by Monte Carlo Conformational Search protocol implemented in Schrodinger Macromodel. The input structure consisted of the ligand and a shell of receptor amino acids within the specified distance (6 Å) from the ligand. A second external shell of all the residues within a distance of 8 Å from the first shell was kept fixed. During the Monte Carlo conformational searching, the input structure was modified by random changes in user-specified torsion angles (for all input structure residues), and molecular position (for the ligand). Hence, the ligand was left free to be continuously re-oriented within the binding site and the conformation of both ligand and internal shell residues could be explored and reciprocally relaxed. The method consisted of 10,000 Conformational Search steps with MMFF94s force field.44, 45, 46, 47, 48, 49, 50 For each A2AAR-based model, the best hA3AR–MRS 1220 complex was saved. The four final complexes served as input in MOE and were subjected to energy minimization with the same protocol as above. This protocol was recently used to prepare hA3AR models for docking and dynamics studies of nucleoside agonists at the same receptor.41, 51

6.2.3. Molecular docking analysis

All compound structures were docked into the binding site of the four hA3AR models using the MOE Dock tool. This method is divided into a number of stages: Conformational Analysis of ligands. The algorithm generated conformations from a single 3D conformation by conducting a systematic search. In this way, all combinations of angles were created for each ligand. Placement. A collection of poses was generated from the pool of ligand conformations using Triangle Matcher placement method. Poses were generated by superposition of ligand atom triplets and triplet points in the receptor binding site. The receptor site points are alpha sphere centers which represent locations of tight packing. At each iteration a random conformation was selected, a random triplet of ligand atoms and a random triplet of alpha sphere centers were used to determine the pose. Scoring. Poses generated by the placement methodology were scored using two available methods implemented in MOE, the London dG scoring function which estimates the free energy of binding of the ligand from a given pose, and Affinity dG scoring which estimates the enthalpic contribution to the free energy of binding. The top 30 poses for each ligand were output in a MOE database.

6.2.4. Post docking analysis

The five top-score docking poses of each compound were then subjected to AMBER99 force field energy minimization until the RMS gradient of the potential energy was less than 0.05 kJ mol−1 Å−1. Receptor residues within 6 Å distance from the ligand were left free to move, while the remaining receptor coordinates were kept fixed. AMBER99 partial charges of receptor and MOPAC output partial charges of ligands were utilized. Once the compound-binding site energy minimization was completed, receptor coordinates were fixed and a second energy minimization stage was performed leaving only compound atoms free to move. MMFF94 force field was applied. For each compound, the minimized docking poses were then rescored using London dG

and Affinity dG scoring functions and the dock-pKi predictor. The latter tool estimates the pKi for each ligand using the 'scoring.svl' script retrievable at the SVL exchange service (Chemical Computing Group, Inc. SVL exchange: http://svl.chemcomp.com). The algorithm is based on an empirical scoring function consisting of a directional hydrogen-bonding term, a directional hydrophobic interaction term, and an entropic term (ligand rotatable bonds immobilized in binding). The four top-score docking poses according to at least two out of three scoring functions were selected for final ligand-target interaction analysis for each compound.

6.3. Pharmacology

6.3.1. Human cloned A1, A2A, and A3 AR Binding Assay

Binding experiments at hA1 and hA2A ARs, stably expressed in CHO cells, were performed as previously described,52 using [3H]DPCPX and [3H]NECA, respectively, as radioligands. Displacement of [125I]AB-MECA from hA3 AR, stably expressed in CHO cells, was performed as reported in Ref. 53.

6.3.2. A2B AR functional assay

Intracellular cyclic AMP (cAMP) levels were measured using a competitive protein binding method.54 CHO cells, expressing recombinant human A2BARs, were harvested by trypsinization. After centrifugation and re-suspension in medium, cells (~30,000) were plated in 24-well plates in 0.5 mL of medium. After 24 h, the medium was removed, and the cells were incubated at 37 °C for 15 min with 0.5 mL of Dulbecco's Modified Eagle Medium (DMEM) in the presence of adenosine deaminase (ADA) (1 U/mL) and the phosphodiesterase inhibitor Ro20-1724 (20 μM). The pharmacological profile of the compounds towards A2B ARs was evaluated by assessing cAMP accumulation in the absence or presence of the agonist NECA

(100 nM). Cells were incubated in the reaction medium (15 min at 37 °C) with the target compounds (10 μM) and then were treated with the agonist.

Following incubation, the reaction was terminated by the removal of the medium and the addition of 0.4 N HCl. After 30 min, lysates were neutralized with 4 N KOH, and the suspension was centrifuged at 800 g for 5 min. For the determination of cAMP production, bovine adrenal cAMP binding protein was incubated with [3H]cAMP (2 nM) and 50 μL of cell lysate or cAMP standard (0–160 pmol) at 0 °C for 150 min in a total volume of 300 μL. Bound radioactivity was separated by rapid filtration through GF/C glass fiber filters and washed twice with 4 mL 50 mM Tris–HCl, pH 7.4. The radioactivity was measured by liquid scintillation spectrometry.

6.3.3. Data analysis

The concentration of the tested compounds that produced 50% inhibition of specific [3H]DPCPX, [3H]NECA, [125I]AB-MECA, [3H]CHA and [3H]CGS 21680 binding (IC50) was calculated using a non-linear regression method implemented by the InPlot program (Graph-Pad, San Diego, CA, U.S.A.) with five concentrations of displacer, each performed in triplicate. Inhibition constants (Ki) were calculated according to the Cheng–Prusoff equation.55 The Kd values of [3H]DPCPX, [3H]NECA and [125I]AB-MECA in hA1, hA2A and hA3 ARs in CHO cell membranes were 3 nM, 30 nM and 1.4 nM, respectively. The dissociation constant (Kd) of [3H]CHA and [3H]CGS 21680 in cortical and striatal bovine brain membranes were 1.2 and 14 nM, respectively.

Acknowledgment

This work was supported by a Grant from the Italian Ministry for University and Research (MIUR, FIRB RBNE03YA3L project).

References

1. Fredholm, B. B.; IJzerman, A. P.; Jacobson, K. A.; Linden, J.; Muller, C. E. Pharmacol. Rev. 2011, 63, 1.
2. Meyerhof, W.; Muller-Brechlin, R.; Richter, D. FEBS Lett. 1991, 284, 155.
3. Salvatore, C. A.; Jacobson, K. A.; Taylor, H. E.; Linden, J.; Johnson, R. G. Proc. Natl.
Acad. Sci. U.S.A. 1993, 90, 10365.
4. Fredholm, B. B.; IJzerman, A. P.; Jacobson, K. A.; Klotz, K. N.; Linden, J. Pharmacol. Rev. 2001, 53, 527.
5. Linden, J. Trends Pharmacol. Sci. 1994, 15, 298.
6. Schulte, G.; Fredholm, B. B. Cell Signalling 2003, 15, 813.
7. Mozzicato, S.; Joshi, B. V.; Jacobson, K. A.; Liang, B. T. FASEB J. 2004, 18, 406.
8. Shneyvays, V. D.; Leshem; Zinman, T.; Mamedova, L. K.; Shainberg, K. A.; Jacobson, A. Am. J. Physiol. Heart Circ. Physiol. 2005, 288, H279.
9. Cheong, S. L.; Federico, S.; Venkatesan, G.; Mandel, A. L.; Shao, Y.-M.; Moro, S.; Spalluto, G.; Pastorin, G. Med. Chem. Rev. 2013, 33, 235.
10. Pugliese, A. M.; Coppi, E.; Volpini, R.; Cristalli, G.; Corradetti, R.; Jeong, L. S.; Jacobson, K. A.; Pedata, F. Biochem. Pharmacol. 2007, 74, 768.
11. Colotta, V.; Catarzi, D.; Varano, F.; Capelli, F.; Lenzi, O.; Filacchioni, G.; Martini, C.; Trincavelli, L.; Ciampi, O.; Pugliese, A. M.; Pedata, F.; Schiesaro, A.; Morizzo, E.; Moro, S. J. Med. Chem. 2007, 50, 4061.
12. Merighi, S.; Benini, A.; Mirandola, P.; Gessi, S.; Varani, K.; Leung, E.; Maclennan, S.; Borea, P. A. Biochem. Pharmacol. 2006, 72, 19.
13. Gessi, S.; Cattabriga, E.; Avitabile, A.; Gafa', R.; Lanza, G.; Cavazzini, L.; Bianchi, N.; Gambari, R.; Feo, C.; Liboni, A.; Gullini, S.; Leung, E.; Mac-Lennan, S.; Borea, P. A. Clin. Cancer Res. 2004, 10, 5895.
14. Gessi, S.; Merighi, S.; Varani, K.; Leung, E.; Mac Lennan, S.; Borea, P. A. Pharmacol. Ther. 2008, 117, 123.
15. Colotta, V.; Cecchi, L.; Catarzi, D.; Filacchioni, G.; Martini, C.; Tacchi, P.; Lucacchini, A. Eur. J. Med. Chem. 1995, 30, 133.
16. Catarzi, D.; Colotta, V.; Varano, F.; Filacchioni, G.; Martini, C.; Trincavelli, L.; Lucacchini, A. Il Farmaco. 2004, 59, 71.
17. Catarzi, D.; Colotta, V.; Varano, F.; Calabri, F. R.; Lenzi, O.; Filacchioni, G.; Trincavelli, L.; Martini, C.; Tralli, A.; Monopoli, C.; Moro, S. Bioorg. Med. Chem. 2005, 13, 705.
18. Catarzi, D.; Colotta, V.; Varano, F.; Lenzi, O.; Filacchioni, G.; Trincavelli, L.; Martini, C.; Monopoli, C.; Moro, S. J. Med. Chem. 2005, 48, 7932.
19. Francis, J. E.; Cash, W. D.; Psychoyos, S.; Ghai, G.; Wenk, P.; Friedmann, R. C.; Atkins, C.; Warren, V.; Furness, P.; Hyun, J. L. J. Med. Chem. 1988, 31, 1014.
20. Jung, K. Y.; Kim, S. K.; Gao, Z. G.; Gross, A. S.; Melman, N.; Jacobson, K. A.; Kim,

Y. C. Bioorg. Med. Chem. 2004, 12, 613.
21. Alanine, A.; Anselm, L.; Steward, L.; Thomi, S.; Vifian, W.; Groaning, M. D. Bioorg. Med. Chem. Lett. 2004, 14, 817.
22. Cosimelli, B.; Greco, G.; Ehlardo, M.; Novellino, E.; Da Settimo, F.; Taliani, S.; La Motta, C.; Bellandi, M.; Tuccinardi, T.; Martinelli, A.; Ciampi, O.; Trincavelli, M. L.; Martini, C. J. Med. Chem. 2008, 51, 1764.
23. Carlsson, J.; Tosh, D. K.; Phan, K.; Gao, Z.-G.; Jacobson, K. A. Med. Chem. Lett. 2012, 3, 715.
24. Catarzi, D.; Colotta, V.; Varano, F.; Poli, D.; Squarcialupi, L.; Filacchioni, G.; Varani, K.; Vincenzi, F.; Borea, P. A.; Dal Ben, D.; Lambertucci, C.; Cristalli, G. Bioorg. Med. Chem. 2013, 21, 283.
25. Morizzo, E.; Capelli, F.; Lenzi, O.; Catarzi, D.; Varano, F.; Filacchioni, G.; Vincenzi, F.; Varani, K.; Borea, P. A.; Colotta, V.; Moro, S. J. Med. Chem. 2007, 50, 6596.
26. Catarzi, D.; Cecchi, L.; Colotta, V.; Melani, F.; Filacchioni, G.; Martini, C.; Giusti, L.; Lucacchini, A. Il Farmaco. 1993, 48, 1065.
27. Zhang, C.-Y.; Liu, X.-H.; Wang, B.-L.; Wang, S. H.; Li, Z.-M. Chem. Biol. Drug Des.
2010, 75, 489.
28. Baumstark, A. L.; Vasquez, P. C. J. Org. Chem. 1983, 48, 65.
29. Gelleri, A.; Messmer, A.; Pinter, I.; Radics, L. J. Prakt. Chem. 1976, 318, 881.
30. Jaakola, V. P.; Ijzerman, A. P. Curr. Opin. Struct. Biol. 2010, 20, 401.
31. Doré, A. S.; Robertson, N.; Errey, J. C.; Ng, I.; Hollenstein, K.; Tehan, B.; Hurrell, E.; Bennett, K.; Congreve, M.; Magnani, F.; Tate, C. G.; Weir, M.; Marshall, F. H. Structure 2011, 19, 1283.
32. Congreve, M.; Andrews, S. P.; Dore, A. S.; Hollenstein, K.; Hurrell, E.; Langmead, C. J.; Mason, J. S.; Ng, I. W.; Tehan, B.; Zhukov, A.; Weir, M.; Marshall, F. H. J. Med. Chem. 1898, 2012, 55.
33. Dal Ben, D.; Lambertucci, C.; Marucci, G.; Volpini, R.; Cristalli, G. Curr. Top. Med.
Chem. 2010, 10, 993.
34. Costanzi, S.; Ivanov, A. A.; Tikhonova, I. G.; Jacobson, K. A. Front. Drug Des. Discov. 2007, 3, 63.
35. Molecular Operating Environment, in, C.C.G. Inc, 1255 University St., Suite 1600, Montreal, Quebec, Canada, H3B 3X3.
36. Kim, Y. C.; Ji, X. D.; Jacobson, K. A. J. Med. Chem. 1996, 39, 4142.
37. Stewart, J. J. J. Comput. Aided Mol. Des. 1990, 4, 1.
38. Dal Ben, D.; Lambertucci, C.; Taffi, S.; Vittori, S.; Volpini, R.; Cristalli, G.; Klotz, K.-N. Purinergic Signalling. 2006, 2, 589.
39. Volpini, R.; Dal Ben, D.; Lambertucci, C.; Taffi, S.; Vittori, S.; Klotz, K.-N.; Cristalli, G. J. Med. Chem. 2007, 50, 1222.
40. Volpini, R.; Buccioni, M.; Dal Ben, D.; Lambertucci, C.; Lammi, C.; Marucci, G.; Ramadori, A. T.; Klotz, K.-N.; Cristalli, G. J. Med. Chem. 2009, 52, 7897.
41. Dal Ben, D.; Buccioni, M.; Lambertucci, C.; Marucci, G.; Thomas, A.; Volpini, R.; Cristalli, G. Bioorg. Med. Chem. 2010, 18, 7923.
42. Mohamadi, F.; Richards, N. G. J.; Guida, W. C.; Liskamp, R.; Lipton, M.; Caufield, C.; Chang, G.; Hendrickson, T.; Still, W. C. J. Comput. Chem. 1990, 11, 440.

43. Cornell, W. D.; Cieplak, P.; Bayly, C. I.; Gould, I. R.; Merz, K. M.; Ferguson, D. M.;
Spellmeyer, D. C.; Fox, T.; Caldwell, J. W.; Kollman, P. A. J. Am. Chem. Soc. 1995, 117, 5179.
44. Halgren, T. A. J. Comput. Chem. 1996, 17, 490.
45. Halgren, T. A. J. Comput. Chem. 1996, 17, 520.
46. Halgren, T. A. J. Comput. Chem. 1996, 17, 553.
47. Halgren, T. A. J. Comput. Chem. 1996, 17, 587.
48. Halgren, T. A. J. Comput. Chem. 1999, 20, 720.
49. Halgren, T. A. J. Comput. Chem. 1999, 20, 730.
50. Halgren, T. A.; Nachbar, R. J. Comput. Chem. 1996, 17, 616.
51. Dal Ben, D.; Buccioni, M.; Lambertucci, C.; Kachler, S.; Falgner, N.; Marucci, G.; Thomas, A.; Cristalli, G.; Volpini, R.; Klotz, K.-N. Biochem. Pharmacol. 2014, 87, 321.
52. Novellino, E.; Cosimelli, B.; Ehlardo, M.; Greco, G.; Iadanza, M.; Lavecchia, A.; Rimoli, M. G.; Sala, A.; Da Settimo, A.; Primofiore, G.; Da Settimo, F.; Taliani, S.; La Motta, C.; Klotz, K.-N.; Tuscano, D.; Trincavelli, M. L.; Martini, C. J. Med. Chem. 2005, 48, 8253.
53. Colotta, V.; Catarzi, D.; Varano, F.; Filacchioni, G.; Martini, C.; Trincavelli, L.; Lucacchini, A. Bioorg. Med. Chem. 2003, 11, 3541.
54. Nordstedt, C.; Fredholm, B. B. Anal. Biochem. 1990, 189, 231.
55. Cheng, Y. C.; Prusoff, W. H. Biochem. Pharmacol. 1973, 22, 3099.

Table 1. Binding affinity (Ki) at hA3, hA1 and hA2A ARs of the 5-substituted 2-aryl-4,5-dihydro-1,2,4-triazolo[1,5-a]quinoxaline derivatives (Series C)

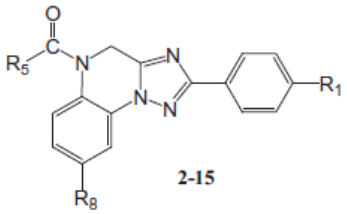

2-15

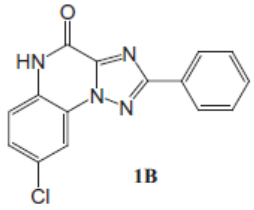

1B

	R_1	R_5	R_8	K_i[a] (nM) or I%		
				hA_3[b]	hA_1[c]	hA_{2A}[d]
2	H	C_2H_5	Cl	72 ± 6.8	39%	24%
3	H	OC_2H_5	Cl	166 ± 15	n.d.	n.d.
4	H	C_2H_5	H	55%	1360 ± 50	52%
5	H	OCH_3	H	245 ± 24	34%	50%
6	H	OC_2H_5	H	22%	4600 ± 118	33%
7	H	C_2H_5	CH_3	6.5 ± 0.5	134.3 ± 7	33%
8	H	OCH_3	CH_3	31.9 ± 3	1481 ± 145	32%
9	H	OC_2H_5	CH_3	12.5 ± 1.1	556 ± 55	9%
10	H	OC_3H_7	CH_3	171 ± 16	565 ± 72	56%
11	OCH_3	C_2H_5	CH_3	25.1 ± 2	1543 ± 61	6%
12	OCH_3	OC_2H_5	CH_3	39.4 ± 3	86 ± 8	2%
13	OCH_3	$OCH_2C{\equiv}CH$	CH_3	23.3 ± 1.8	49%	13%
14	OCH_3	$CH_2C_6H_5$	CH_3	54.8 ± 5	39%	0%
15	OCH_3	$OCH_2C_6H_5$	CH_3	231.4 ± 18	45%	4%
1B[e]	—	—	—	163 ± 13	n.d.	n.d.

[a] Ki values are means ± SEM of four separate assays, each performed in triplicate.
[b] Displacement of specific [125I]AB-MECA binding at hA3 receptors expressed in CHO cells or percentage of inhibition (I%) of specific binding at 1 μM.
[c] Displacement of specific [3H]DPCPX binding at hA1 receptors expressed in CHO cells or percentage of inhibition (I%) of specific binding at 10 μM concentration.
[d] Percentage of inhibition (I%) of specific [3H]NECA binding at hA2A receptors expressed in CHO cells, at 10 μM concentration.
[e] Ref. 18.

Table 2. Binding activity at human A_1, A_{2A} and A_3 adenosine receptors of compounds **16a-i** and **17a-i**

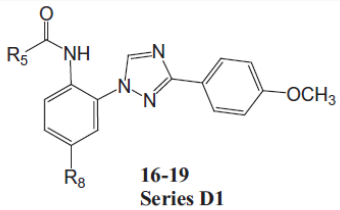

16-19
Series D1

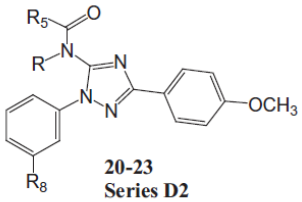

20-23
Series D2

	R	R_5	R_8	K_i[a] (nM) or I%		
				hA_3[b]	hA_1[c]	hA_{2A}[d]
16	–	OC_2H_5	CH_3	34%	6%	13%
17	–	$OCH_2C{\equiv}CH$	CH_3	35%	n.d.	16%
18	–	$CH_2C_6H_5$	CH_3	45%	44%	1%
19	–	$OCH_2C_6H_5$	CH_3	47%	2%	7%
20	$COCH_3$	CH_3	H	19%	26%	4%
21	H	C_6H_5	H	50%	25%	43%
22	COC_6H_5	C_6H_5	H	44%	55%	13%
23	H	NHC_6H_5	H	545 ± 48	1%	7%

a Ki values are means ± SEM of four separate assays, each performed in triplicate.
b Displacement of specific [125I]AB-MECA binding at hA3 receptors expressed in CHO cells or percentage of inhibition (I%) of specific binding at 1 μM.
c Percentage of inhibition (I%) of specific [3H]DPCPX binding at hA1 receptors expressed in CHO cells, at 10 μM concentration.
d Percentage of inhibition (I%) of specific [3H]NECA binding at hA2A receptors expressed in CHO cells, at 10 μM concentration.

Table 3. Binding affinity (Ki) at hA3, hA1 and hA2A ARs of the 1,2,4-triazolo[1,5-a]quinoxaline derivatives (Series E)

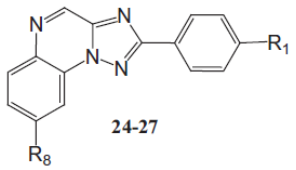

24-27

	R_1	R_8	K_i[a] (nM) or I%		
			hA_3[b]	hA_1[c]	hA_{2A}[d]
24	H	Cl	15.2 ± 1.6	127.4 ± 13	19%
25	H	H	91.5 ± 8.9	n.d.	n.d.
26	H	CH_3	23.9 ± 2.19	1322 ± 135	2401 ± 246
27	OCH_3	CH_3	26.6 ± 1	2016 ± 100	30%

a Ki values are means ± SEM of four separate assays each performed in triplicate.
b Displacement of specific [125I]AB-MECA binding at hA3 receptors expressed in CHO cells.
c Displacement of specific [3H]DPCPX binding at hA1 receptors expressed in CHO cells.
d Displacement of specific [3H]NECA binding at hA2A receptors expressed in CHO cells or percentage of inhibition (I%) of specific binding at 10 μM concentration.

Table 4. Effect of some selected compounds on cAMP production in CHO cells expressing hA2B ARa

	% of cAMP production[b]
2	63.7 ± 4.7
7	68.6 ± 4.6
8	74.9 ± 6.3
9	103.8 ± 5.1
11	102.4 ± 6.7
13	108.9 ± 10.2
14	89.5 ± 8.3
27	42.6 ± 1.9

a The effect of each compound at 10 μM concentration was evaluated. Each compound was tested in the presence of an EC50 concentration of agonist NECA (100 nM, determined on the same day as each assay).
b Data are expressed as percentage of cAMP production versus agonist set to 100%. All data represent the mean ± SEM of two different experiments each performed in duplicate.

Captions

Scheme 1. Reagents and conditions. (a) LiAlH4, anhydrous tetrahydrofuran, nitrogen atmosphere, reflux; (b) glacial acetic acid, reflux; (c) R5COCl, pyridine, anhydrous dichloromethane, nitrogen atmosphere; (d) ClCOCH2Cl, anhydrous toluene, 80 °C; (e) SnCl2 dihydrate, ethanol, reflux.

Scheme 2. Reagents and condition: (a) CH(OEt)3, p-toluensulfonic acid, 100 °C; (b) 10% Pd/C, H2, ethyl acetate; (c) R5COCl, pyridine, anhydrous dichloromethane, 0 °C.

Scheme 3. Reagents and condition. (a) POCl3, PCl5, reflux; (b) NH2CN, 100 °C; (c) acetic anhydride, pyridine, reflux; or C6H5COCl, pyridine, anhydrous tetrahydrofuran, reflux; or C6H5NCO, anhydrous dichloromethane, 5 °C/room temperature.

Figure Legend

Figure 1. Figure 1. Previously reported 4-amino- and 4-oxo-substituted 2-(hetero)aryl-1,2,4-triazolo[1,5-a]quinoxaline (TQX) derivatives as human A3 adenosine receptor antagonists.

Figure 2. Currently reported 1,2,4-triazolo[1,5-a]quinoxaline (TQX) derivatives and their simplified 1,3-diaryl-1,2,4-triazole analogues.

Figure 3. Panel A. Family 1 docking conformations. The binding mode of compound 7 at 3EML-based hA3AR model is shown as example. Panels B and C. Detailed view of ligand-target interaction considering the 8- and the 5-substituent, respectively.

Figure 4. Panel A. Family 2 docking conformations. The binding mode of compound 7 at 3EML-based hA3AR model is shown as example. Panels B and C. Detailed view of ligand-target interaction considering the 5- and the 8-substituent, respectively.

Figure 5. Panel A. Superimposition of family 1 (light) and 2 (dark) docking conformations. The binding mode of compound 7 at 3EML-based hA3AR model is shown as example. The superimpositions of 5- and 8-substituents (I and II) and 2-substituents (III) are highlighted. Panel B. Docking conformations of simplified triazoles (compound 23) at 3EML-based hA3AR model.

Scheme 1

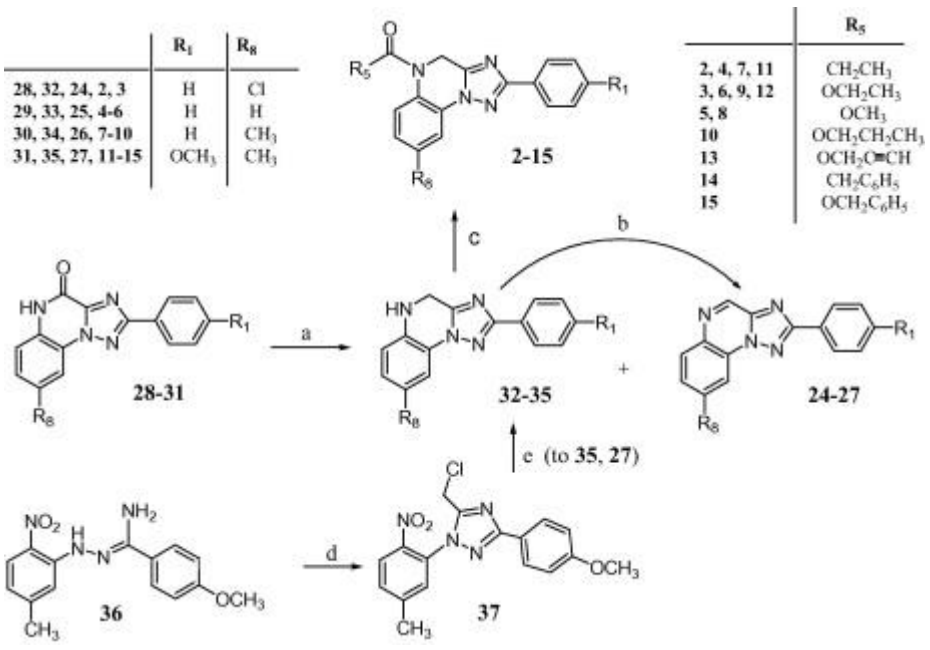

Scheme 2

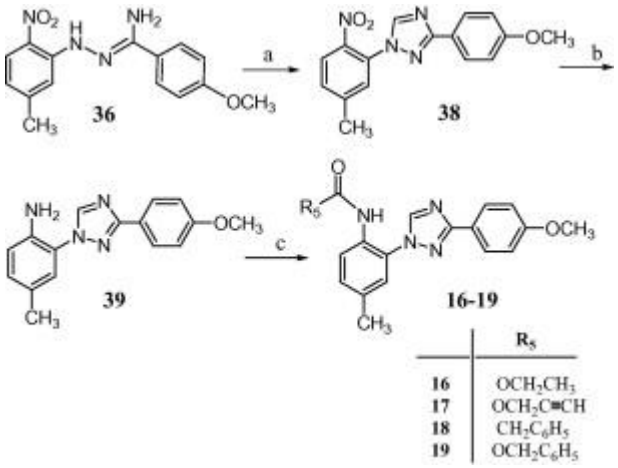

	R_5
16	OCH_2CH_3
17	$OCH_2C{\equiv}CH$
18	$CH_2C_6H_5$
19	$OCH_2C_6H_5$

Scheme 3

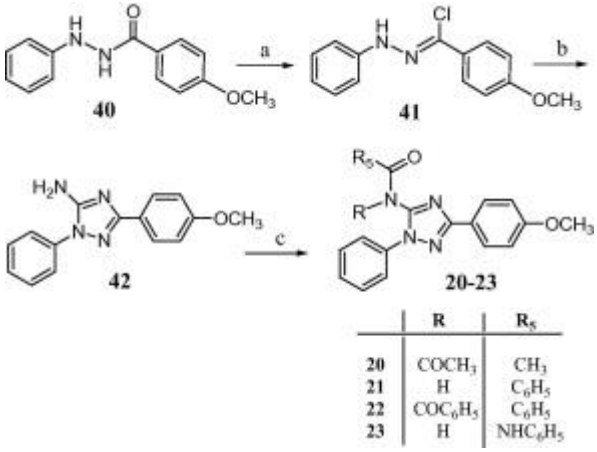

	R	R_5
20	$COCH_3$	CH_3
21	H	C_6H_5
22	COC_6H_5	C_6H_5
23	H	NHC_6H_5

Figure 1

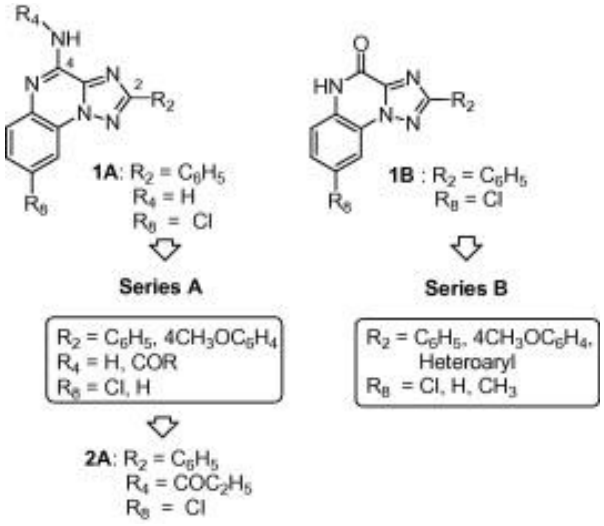

Figure 2

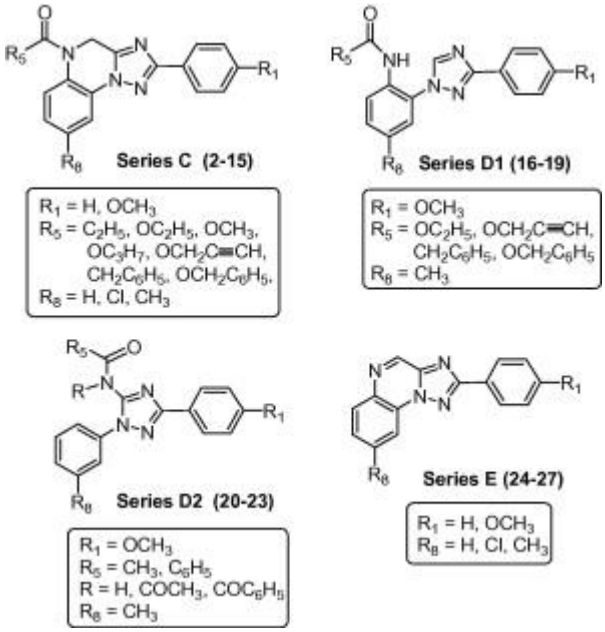

Figure 3

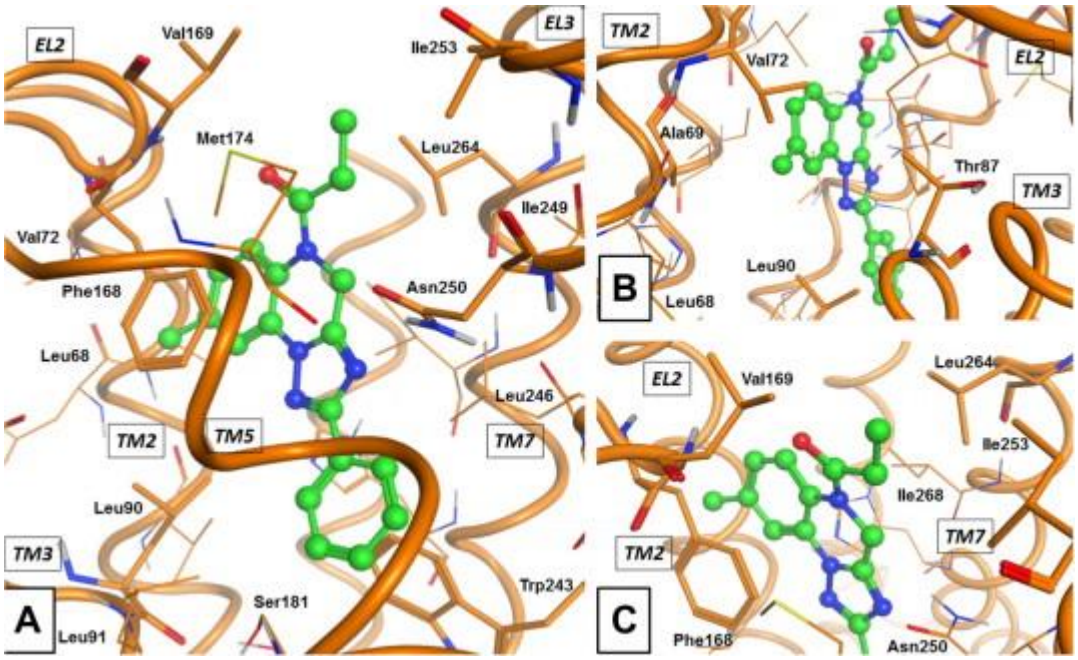

Figure 4

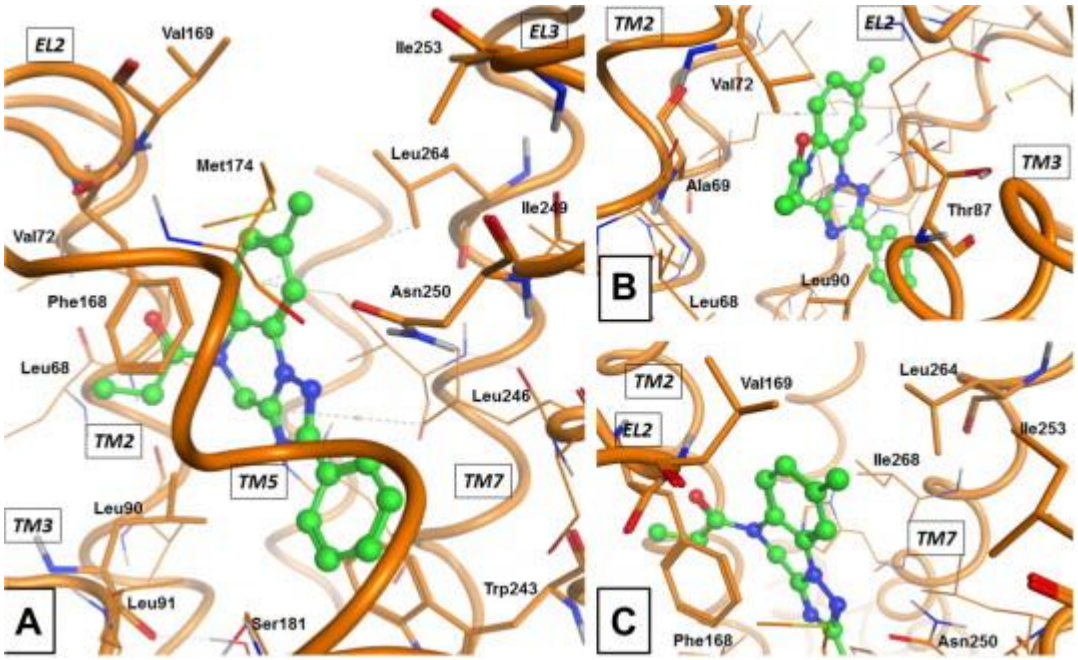

Figure 5

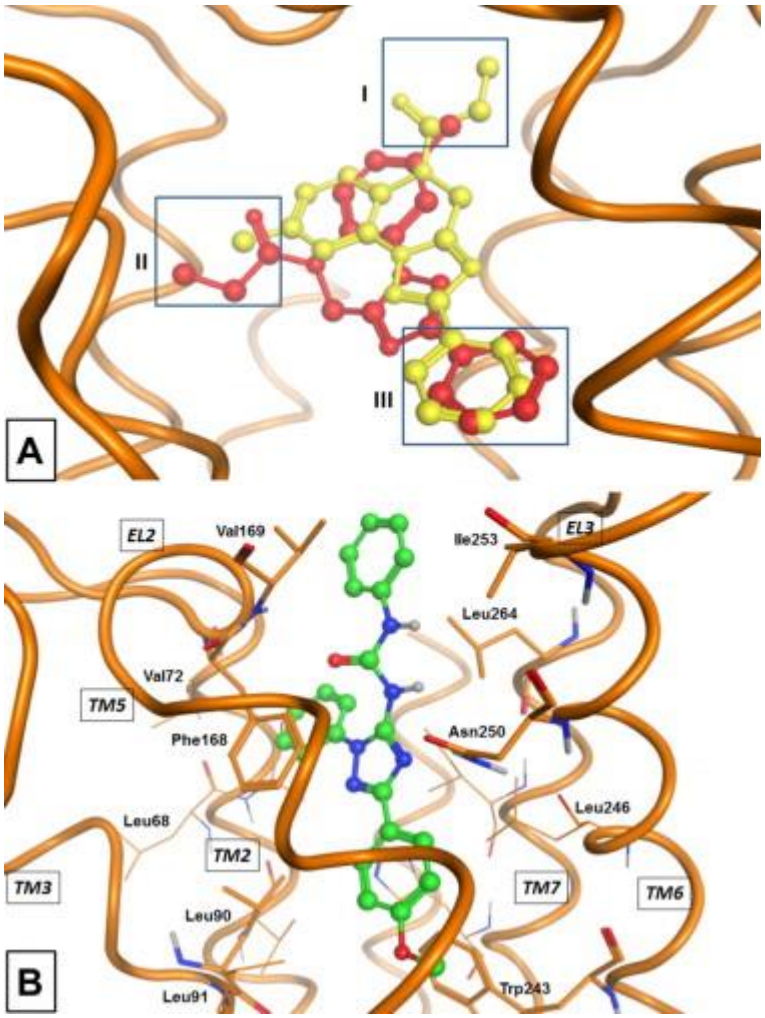
I
II
III
A
EL2
Val169
Ile253
EL3
Leu264
Val72
TM5
Phe168
Asn250
Leu246
Leu68
TM2
TM3
TM7
TM6
Leu90
Leu91
Trp243
B